Fisheries Research 243 (2021) 106067

Contents lists available at ScienceDirect

Fisheries Research

journal homepage: www.elsevier.com/locate/fishres

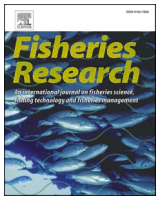

Full length article

# Use of manned submersible and autonomous stereo-camera array to assess forage fish and associated subtidal habitat

Matthew R. Baker [a,b,*], Kresimir Williams [a], H.G. Greene [c,d], Casey Greufe [b], Heather Lopes [b], John Aschoff [d], Rick Towler [a]

[a] Alaska Fisheries Science Center, National Oceanic and Atmospheric Administration, Seattle, WA, USA
[b] University of Washington, School of Aquatic and Fishery Science and Friday Harbor Laboratories, WA, USA
[c] Moss Landing Laboratories, California Status University, Monterrey, CA, USA
[d] Tombolo Mapping Laboratory, Orcas Island, WA, USA

ARTICLE INFO

Handled by George A. Rose

*Keywords:*
*Ammodytes* spp.
Visual data
Underwater imaging
Sediment
Dynamic bedforms
Fishery-independent surveys

ABSTRACT

Forage fish and fish associated with particular benthic habitats (e.g., rockfishes, sand eels, sand lances) may be particularly difficult to assess through standard survey methodologies. Stereo-cameras, video, and automated visual data may serve as useful complementary tools to provide insight into the dynamics of these species. Visual methods may be used not only to estimate abundance and distribution, but also to inform important biological metrics and life history attributes. We explored the application of these methods to assess Pacific sand lance (*Ammodytes personatus*), a forage fish associated with benthic sediments, using a combination of directed observations from a manned submersible and quantitative analysis of fixed image footage obtained with a stereo-camera. This research provides a better understanding of how *in situ* observations and automated image analysis might complement other methods to estimate fish abundance, distribution, habitat, and behavior. Visual data were compared to data collected via directed sampling using physical extraction methods at the same site in the same year. Submersible observations provided new insights on the physical conditions and habitat. Visual observations confirmed wavefield morphologies previously identified through multibeam acoustic imagery and measured attributes relevant to the physical oceanography of the water column above this benthic habitat feature. Visual observations also informed understanding of light penetration, relevant to diurnal cues for seasonal progression and diel vertical migration and foraging. Submersible observations provided insights into abundance, schooling dynamics, and behavioral attributes, including avoidance in response to physical disturbance and aggregation in presence of artificial light. Quantitative analysis of stereo-camera data in center-edge and north-south transects determined that fish abundance and length distribution was relatively uniform throughout this particular benthic habitat. Estimates of measurement error associated with stereo-cameras were calculated and correction factors identified. Mean lengths estimated in visual data and in physical specimens were closely matched, though variance in visual data measurements was far greater. This error was reduced when filtering data on the basis of orthogonal position or incidence angle relative to the camera. Our research provides important insights to the presence, distribution, abundance, and movement of Pacific sand lance within benthic sand wavefield habitats. Our research also provides insight to the applications, opportunities, and constraints to observation-based sampling methods, including the use of manned submersibles and automated stereo-cameras.

## 1. Introduction

Effective monitoring of pelagic marine fish populations may require a variety of assessment methods (Boldt et al., 2017, 2018, 2019; Baker et al., 2018; Moriarty et al., 2020). Standardized abundance indices based on catch and effort indices and fishery-dependent data are a fundamental input to stock assessments (Hilborn, 1979; Maunder and Punt, 2004; Bishop, 2006), but fishery-dependent data may be of limited utility in monitoring non-target species or non-target areas (Thorson and Ward, 2014; Thorson et al., 2016). Surveys and other traditional

* Corresponding author at: Alaska Fisheries Science Center, National Oceanic and Atmospheric Administration, Seattle, WA, USA.
*E-mail address:* Matthew.Baker@noaa.gov (M.R. Baker).

https://doi.org/10.1016/j.fishres.2021.106067
Received 4 February 2021; Received in revised form 12 May 2021; Accepted 3 July 2021
Available online 10 July 2021

fishery-independent assessment methods (Hilborn and Walters, 2013) provide more comprehensive indices of system biomass (Sainsbury et al., 2000; Koslow and Davison, 2016), species distribution (Baker and Hollowed, 2014; Moriarty et al., 2020) and species dynamics (Gaichas et al., 2010; Karp et al., 2019). These methods, however, may be spatially limited (Link et al., 2011), biased in their target or design (Thorson et al., 2016), ineffective in certain habitats (Baker et al., 2019a) or constrained in accurately assessing certain types of fishes, particularly pelagic and forage fishes (Fréon and Misund, 1999; Alheit and Peck, 2019). Estimating fish biomass is particularly challenging where catchability or availability of fish to survey gear is limited (Ward, 2008). Estimating biomass and abundance is further complicated where the distribution of the species is restricted to specific habitats (Millar and Methot, 2002) or the species of interest is characterized by patchiness in spatial or temporal distribution (Thorson et al., 2011; Boyd et al., 2015).

Fish are temporally and spatially variable in their abundance and distribution, particularly forage fish (Fréon and Misund, 1999; Greene et al., 2015; Baker, 2021). This may restrict their availability to surveys (McGowan et al., 2019). Fish species with specific habitat-specific associations, such as rockfish, also pose a particular challenge (Spencer and Ianelli, 2014). Often alternative methods are required (Clarke et al., 2009; Rooper et al., 2010; Honkalehto et al., 2011; Hanselman et al., 2012). Remotely operated vehicles (ROVs; Brodeur, 2001; Auster et al., 2003), autonomous underwater vehicles (AUVs; Tolimieri et al., 2008) and human-occupied submersibles (Stein et al., 1992; Starr et al., 1996; Yoklavich et al., 2000; Nasby-Lucas et al., 2002; Rodgveller et al., 2011; Pacunski et al., 2008, 2013) have demonstrated utility in assessing fish abundance and fish habitat. We used a manned submersible (Fig. 1a) and an attached stereo-camera system (Fig. 1b) to enumerate, measure, and observe habitat interactions for an unassessed sand-associated North Pacific forage fish at a deep-water sand wavefield in the Salish Sea.

Our study focuses on Pacific sand lance (PSL; *Ammodytes personatus,* Orr et al., 2015), an ecologically important forage fish distributed throughout the North Pacific Ocean (Appendix, Fig. A-1). Relatively little is known about this species in contrast to commercially valuable North Pacific forage fish such as Pacific herring, sardines, and anchovies (Liedtke et al., 2013). PSL are also distinguished from other common northern latitude forage fish species in their reliance on bottom sediments for refuge (Bizzarro et al., 2016). The San Juan Archipelago in the Salish Sea has a complex bathymetry influenced by previous glaciation (Greene and Barrie, 2011) and provides habitat for what is likely a very significant number of PSL (Greene et al., 2011, 2020; Baker et al., 2021b, In Review). The region is characterized by strong currents, significant oceanic inputs and upwelling (Thomson and Ware, 1996) and is also important habitat to hundreds of species of birds, mammals, and fishes, many of which rely on PSL as a prey resource (Gaydos et al., 2008; Gaydos and Pearson, 2011; Pietsch and Orr, 1999).

An extensive sampling effort conducted by Selleck et al. (2015) found PSL along 82 % of sampled shoreline in the San Juan Islands and the Strait of Georgia. In addition to nearshore populations, Greene and Pacunski (unpublished; 2004) discovered a subtidal sand wave field, during a Washington Department of Fish and Wildlife (WDFG) remotely operated vehicle (ROV) video survey. This San Juan Channel sand wave field has been extensively studied and determined to be an important habitat for PSL (Greene et al., 2017, 2020; Baker et al., 2019b; Baker et al., 2021b, In Review). It is estimated to provide benthic habitat for as many as 100 million PSL (Sisson and Baker, 2017) ages 0–4 years (Matta and Baker, 2020). Many benthic sediments with similar sediment features in the area have since been identified as potential PSL habitat (Greene et al., 2011; Baker, unpublished data).

Since 2010, the Pelagic Ecosystem Function research apprenticeship [http://courses.washington.edu/pelecofn/index.html] at the University of Washington Friday Harbor Laboratories, WA, USA has been focused on studies of PSL at this site (Newton et al., 2018, 2019). Sampling has largely involved sampling PSL with a Van Veen grab. This method has been useful for securing fish and answering questions about sediment association (Baker et al., 2021b, In Review), length-at-age analyses (Matta and Baker, 2020), and demographics and annual condition (Baker et al., 2019b). While successful and efficient in securing fish at known benthic sites (Høines and Bergstad, 2001; Hassel et al., 2004; Greenstreet et al., 2010), sampling by means of Van Veen has limitations. The probability of Van Veen closure is restricted to certain sediment types because large-sized sediment may prevent closure of the device. Additionally, Van Veen grabs are limited to the top layer of sediment (< 22 cm). These methods are also restricted to periods of time when the fish are dormant in sediments, rather than active in the water column. Most importantly, these methods do not allow for observation of fish behavior, response to disturbance, movement between the benthos and the water column, schooling dynamics, physical dynamics related to sediment movement, or analysis of environmental conditions at depth.

In many pelagic fishes, abundance and distribution are effectively monitored and analyzed through acoustic methods (Horne, 2000; Gauthier and Horne, 2004). Unlike most pelagic fishes, however, sand lance and sand eels (*Ammodytes* spp.) lack swim bladders and their acoustic properties are very different than other pelagic fish species (Mosteiro et al., 2004). Specifically, these fish have relatively low target strength values (Forland et al., 2014), which are necessary for accurate acoustic measurements. Acoustic approaches have been applied in the Atlantic (Hassel et al., 2003; Mackinson et al., 2005; Johnsen et al., 2009); however, as sand lance and sand eel form compact schools with

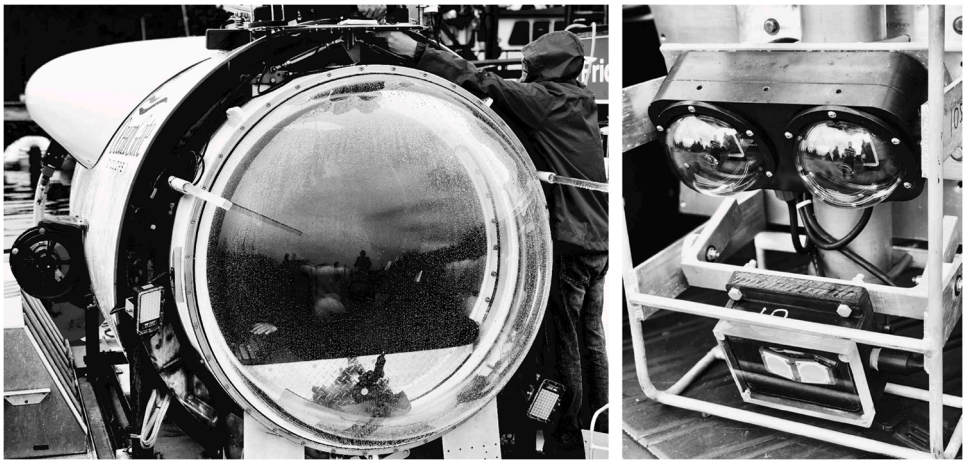

**Fig. 1.** OceanGate Inc. Cyclops I submersible (left); NOAA National Marine Fisheries Service stereo-camera array (right).

low reflectance (weak acoustic backscatter) and are often distributed near-bottom, acoustic methods are limited in their effectiveness and resolution (Ona and Mitson, 1997). In the Northeast Atlantic, where sand eel support one of the most important commercial fisheries by volume (ICES, 2018), pelagic trawls and dredges are used to measure relative densities of these fish in the seabed (Jensen, 2001; van der Kooij et al., 2008). Here too, there are issues of catchability, both in survey trawls (Fraser et al., 2007) and dredge tows (Mackinson et al., 2005; van Deurs et al., 2012). There is international demand for fishery-independent data to improve abundance estimation (Kubilius and Ona, 2012) and to inform management of forage species (ICES, 2008). Current limitations to effective sampling of these fish motivate our efforts to explore and apply new methods.

As an alternative assessment method, stereo-camera surveys have been successfully applied to assess abundance and distribution and to conduct fish length measurements (Harvey et al., 2003; Watson et al., 2005; Shortis et al., 2009; Williams et al., 2016b; Boldt et al., 2018). Fish measurements obtained from stereo-camera imagery have been shown to be accurate (Harvey et al., 2003; Seiler et al., 2012). In addition to developing estimates for fish abundance and morphological metrics, fish behavior can be observed (Somerton et al., 2017). Stereo-camera imagery allows for continuous sampling through space and time as stereo-camera systems can be used on fixed stationary platforms. Operated from submersibles, stereo-cameras may be combined with direct observation to quantify observed dynamics, metrics, and behaviors. Used either in isolation or in combination with other approaches, stereo-cameras can provide a unique perspective and insights, particularly on species difficult to assess through alternative methods.

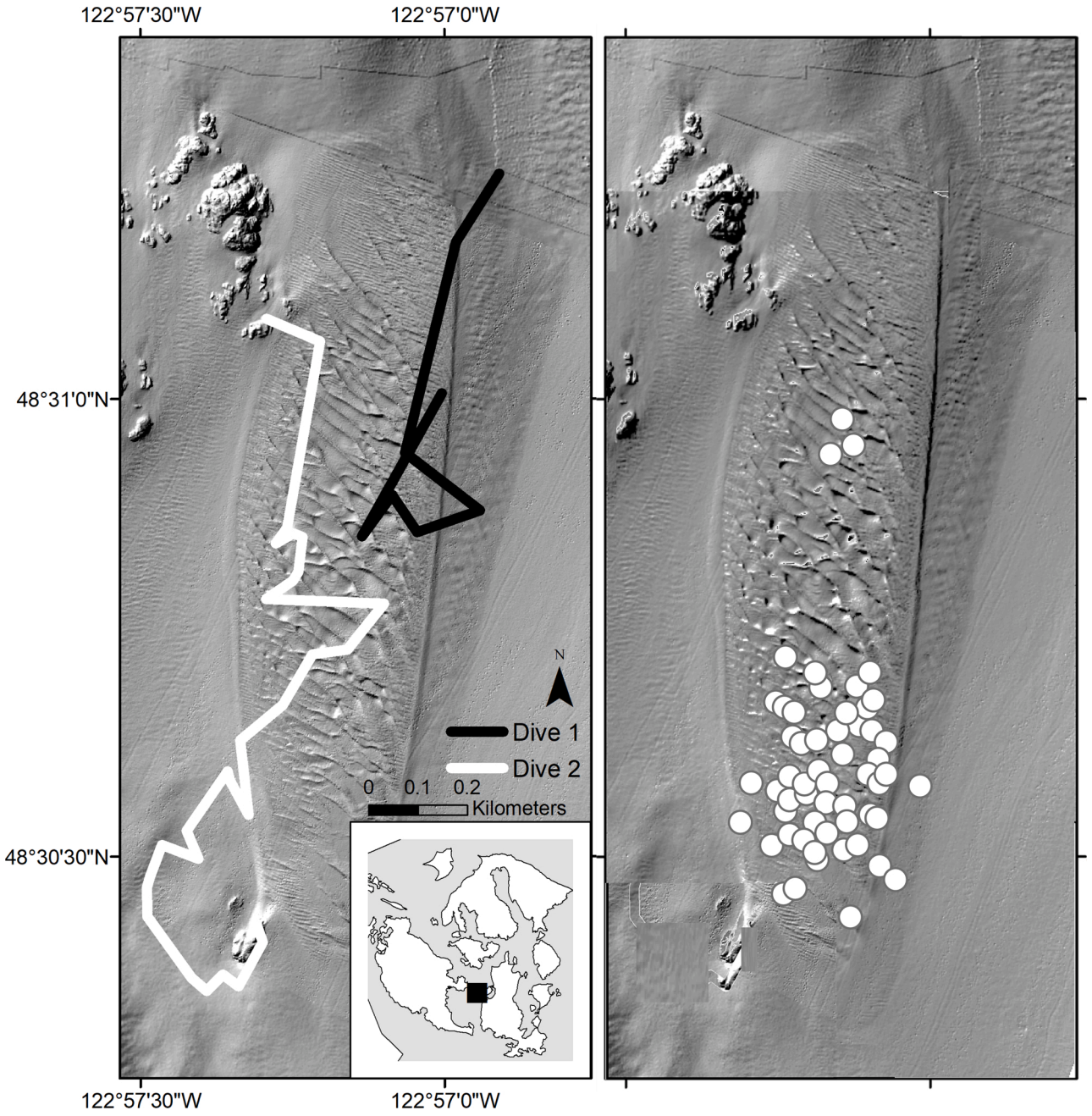


**Fig. 2.** Map of the San Juan Channel sand wave field and two submersible transects in OceanGate Cyclops I, where Pacific sand lance were observed (left panel). Map of sample locations for a series of Van Veen sediment grabs between September 10, 2018 and December 2, 2018, where Pacific sand lance were collected (right panel). Multibeam bathymetry source, see Greene and Barrie, 2011].

We applied stereo-camera data from submersible surveys in concert with Van Veen grab sampling methods to integrate and contrast these approaches and gain greater insight to sources of error associated with each approach. By applying multiple methods at a common site, we provide insight to the behavior, abundance, and attributes of an important, but poorly understood forage fish in the North Pacific. We also introduce potential approaches and correction factors to address bias in stereo-camera morphometric measurement estimates related to fish orientation and suggest improvements in the application of stereo-camera arrays and submersible survey efforts.

## 2. Materials and methods

### 2.1. Study site

PSL were collected or observed at the San Juan Channel (SJC) sand wavefield (48° 31′ N, 122° 57′ W; Fig. 2) in the Salish Sea, Washington, USA. The sand wavefield covers an area of approximately 600,000 $m^2$ and is oriented north-south. The sand wavefield is approximately 0.74 km wide (east-west) and 1.88 km long (north-south) at a depth of 60 m in the north and 80 m at the southern extent. This wavefield contains bedforms with wavelengths up to 100 m and heights of approximately 1–4 m within its central area. It is sharply bounded with definitive edges of the field, maintained by strong tidal currents (Greene et al., 2017). The sand wavefield is a known habitat for adult PSL (Greene et al., 2011, 2017, 2020, 2021; Sisson and Baker, 2017; Baker et al., 2019b; Baker et al., 2021b, In Review). Research at the University of Washington Friday Harbor Laboratories has surveyed PSL from the SJC sand wave field in multiple years (2006, 2010–2020).

### 2.2. Sand wave field physical attributes – multibeam bathymetric imaging

Prior to the submersible survey, multibeam echosounder surveys (MBES) were conducted as part of a collaboration between the Geological Survey of Canada, Canadian Hydrographic Service, Center for Habitat Studies, Moss Landing Marine Labs, and Tombolo/Sea Doc Society. These marine geophysical surveys acquired wide swath MBES bathymetry and backscatter throughout the Northwest Straits region of the Salish Sea (southern Gulf Islands and the San Juan Archipelago). These data along with side-scan sonar mosaics and 3.5 kHz sub-bottom seismic-reflection profiles were used to produce habitat types (Greene et al., 2007) and have subsequently been published in a marine benthic habitat map series (Greene et al., 2011, 2020). These data were also used to produce seafloor images of the sediment wave field for this investigation. MBES bathymetric maps were analyzed and used to identify unique subsections of the wave field based on depth, wave height and length, and bedform slope. Five unique sections along the north-south latitudinal gradient were identified as comparison indices for PSL length and abundance.

### 2.3. Van Veen sampling of sediments

PSL were sampled from the sand wavefield using a Van Veen grab (0.12 $m^2$ surface area). A total of 402 PSL were collected in a total of 67 Van Veen grabs, completed across a series of seven research cruises. Research cruises were conducted between September 10, 2018 and December 2, 2018 on the University of Washington Friday Harbor Laboratories R/V Centennial or R/V Auklet. Captured fish were brought back to the Friday Harbor Laboratories, Washington, USA for total length measurement.

### 2.4. Submersible – OceanGate Cyclops I

The OceanGate Cyclops I manned submersible (https://www.oceangate.com/pdf/oceangate-cyclops-1.pdf; Fig. 1a) was used to conduct sampling along a set of transects (Fig. 2). Cyclops I operated with an enhanced automated control system designed by the University of Washington Applied Physics Lab and OceanGate engineering, using a combination of commercial off-the-shelf technology and innovative system architecture to monitor life support, power management, navigation and other system diagnostics. The dimensions of the submersible were 6.64 m × 2.83 m × 2.17 m at a weight of 9525 kg and payload of 522 kg. This vessel is capable of diving to depths of 500 m and speeds of 2 knots, using a propulsion system of four Innerspace 1002 electric thrusters. Viewing was facilitated through a 1.45 m acrylic front-facing dome, providing a 180-degree field of view with minimal distortion. Navigation was provided through iXblue PHINS Inertial Navigation System and Teledyne BlueView 2D and 3D sonar. Submersible lighting was provided through two Teledyne Bowtech LEDs (40,000 lumens total output).

### 2.5. Stereo-camera configuration

Stereoscopic camera arrays developed by Williams et al. (2018) were bolted to the Cyclops I submersible and used to gather non-lethal *in situ* data on PSL. The system consisted of a camera housing, a strobe light, and a battery, all secured in a metal instrument cage (Fig. 1b). The main housing contained two Chameleon3 machine vision cameras, a single-board ARM (Acorn RISC Machine, Acorn Computers Ltd.) system-on-chip computer (ODroid XU4), and a custom circuit for power and timing control of strobe pulses. Cameras were mounted in a customized aluminum housing manufactured by Sexton Inc. (Salem, OR). Domed viewports were used to allow wide view angles and minimize radial distortion caused by light refraction through flat viewports. The strobe housing was manufactured from 51 mm acetal plastic, using a flat acrylic 19 mm (0.75″) back plate to allow light transmission from the LED elements. The strobe unit consisted of two Bridgelux LED arrays powered by a TaskLED driver, producing approximately 1300 lumens at 10.4 W. The system was powered independent of the submersible using a 24 V 10 Ah NiMH battery pack. The camera, computer strobe light, and battery pack were contained within a protective aluminum housing unit installed on the front of the submersible. Synchronous images were collected from each of the cameras at a frequency of 1 image every 5 s.

### 2.6. Submersible transects and stereo-camera deployments

OceanGate Cyclops I submersible dive transects with the mounted stereo-camera array were conducted on September 10, 2018 (Dive 1) and September 13, 2018 (Dive 2) within the boundaries of the SJC sand wave field (Fig. 2, left panel). The duration of the dive transects were 180 min and 100 min, respectively. Each dive included an east-west subsection to examine center-edge effects, as well as north-south sub-sections to examine depth gradient effects. Full transects of the entire wavefield on each dive were not possible, as each dive limited in spatial extent by both time constraints and current flow. A subsection of dive 2, included a 20-minute 400 m east-west transect from the center of the wave field to the western edge (Appendix, Fig. A-2) to examine variation related to sand wave type, wave period, and sediment type. Dive 1 also included extended periods of stationary time on bottom for the purposes of observation. The stereo-camera array captured images at five second intervals for the duration of both dives. GPS coordinates were recorded intermittently for dive transects and were synced with image time stamps to provide spatial scales on which to compare recorded fish length and abundance. Images were analyzed to measure fish length and observe schooling behavior. A Blackmagic Pocket Cinema 4 K (4096 × 2160 resolution) video camera outfitted with a Panasonic Leica DG 15 mm F1.7 lens was also deployed in the observation dome of the submersible. Ingested video was analyzed, marking one-minute periods. This was used to determine when the submersible was in active motion, resting on the seafloor for observation, and the duration of periods during which submersible lights were turned off to facilitate observation in natural conditions.

Since a primary intent of this research was to evaluate the effects of submersible dives on the ability to estimate abundance, we deliberately included periods of inactivity as well as active motion, included periods of observation with and without light, and deliberately noted where submersible contact with the bottom caused disturbance to benthic substrates. Explicit attention was also made to determine what attributes of these dives provided unique insights to the physical system (e.g., light, visibility) and fish behavior (e.g., avoidance, dispersal, schooling dynamics, response to disturbance of benthic substrates and response to light and noise) that might complement other forms of directed sampling of these fish and this habitat.

### 2.7. Stereo-camera image analysis

Prior to deployment, the cameras were calibrated following methods described in Williams et al. (2010), using the Matlab Camera Calibration Toolbox (Bouguet, 2014). The calibration procedure corrected for distortion of the images due to the lens and viewport optics, as well as solving for the epipolar geometry between the two cameras. Upon completion of the dives, the data collected during a deployment were transferred to a computer over a Wi-Fi link. Analysis of each image pair was used to quantify individual fish along each dive transect using SEBASTES. SEBASTES is an open-source stereo image software package written in Python and developed for the explicit purpose of underwater fish measurement from stereo still images (Williams et al., 2016a; Williams et al., 2016b). More on the software is available [https://repository.library.noaa.gov/view/noaa/11999].

All observed fishes were identified to species level, and all PSL visible were identified and counted. PSL with heads and caudal fins clearly visible in both left and right image frames were measured using the SEBASTES measurement function. Where measurements could not be made due to occlusion or poor visibility, PSL range from the camera was estimated by identifying distinct points on each fish such as the fish eye. PSL that were seen in one image frame and not the other were used in count data only.

### 2.8. Length measurements and error estimation

Fish lengths were measured by using stereo triangulation functions integrated with the camera calibration software package (Bouguet, 2014), which leverage the epipolar geometry of the cameras to estimate the three-dimensional location of each corresponding point seen simultaneously in both cameras (Fig. 3). Length measurements were obtained by identifying the pixel coordinates of the corresponding features of interest in the left and right camera still frames, identifying the forward point of the head and the tail (Fig. 4). These points were used to solve for the three-dimensional coordinates of the points in the images, using calibration-derived parameters. Following identification of the three-dimensional coordinates of the fish endpoints, length was then estimated as the Euclidian distance between the points in real space.

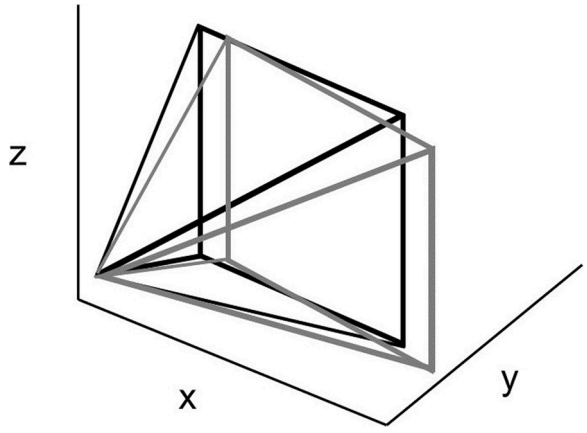


**Fig. 3.** Triangulation methods used to develop position and length measurements in the stereo-camera. Gray projection surface represents the right camera, black projection surface represents the left camera.

A primary intent of this research was to evaluate methodology and error related to the stereo-camera estimates of length estimation. As a result, analysis was conducted in two phases. Initially all stereo-camera measurements were included in the analysis. Subsequently a correction factor was estimated and subsequently used to explicitly account for measurement error, specifically related to the incidence angle (i.e., deviation of fish position from orthogonal relative to the camera). Measurement error in length estimation in the original data was estimated as a function of both distance of the fish from the camera and position of the fish as a function of angle deviance from an orthogonal position to the camera. To determine clear breakpoints, standard deviation for length measurements were binned into 5 degree intervals and a two-segment regression or piecewise regression was applied to the standard deviation of the length measurements for these 5 degree bins. Segmented linear regression with segments separated by a breakpoint can be useful to quantify an abrupt change of a response function (Muggeo, 2003, 2008). Breakpoints can be interpreted as a threshold value beyond or below which undesired effects occur or error increases. Breakpoints were identified through the least squared method applied separately to each segment, by which the two regression lines were made to fit the data set as closely as possible while minimizing the sum of squares of the differences (Muggeo, 2008).

Volumetric fish density was estimated for frames where the seafloor was not seen in the images. The imaging volume was computed using methods developed by Williams et al. (2018).

### 2.9. Environmental data

A Teledyne RD Instruments Citadel TS-NH thermosalinograph was encased in a urethane mold and sealed housing [http://www.teledynemarine.com/ctds] and installed on the submersible. This flow-through system was designed for installation on underwater vehicles and uses a NXIC (Non-eXternal Inductive Conductivity) sensor and an aged thermistor to provide precise conductivity salinity [accuracy, ±0.015 PSU] and temperature measurements.

## 3. Results

### 3.1. Submersible transects and Van Veen sampling

OceanGate Cyclops I was used to conduct two dives at the SJC sand wave field (Fig. 2, left panel). Sample locations for a series of Van Veen sediment grabs between September 10, 2018 and December 2, 2018 are indicated (Fig. 2, right panel).

### 3.2. Physical system

The high abundance and widespread distribution of PSL throughout the San Juan Channel sediment wave field confirm this as an extensive sub-tidal deep-water habitat feature for PSL, an important forage fish in the Salish Sea and throughout the North Pacific. This field contains bedforms with wavelengths up to 100 m and heights of approximately 1–4 m. The sand waves in the San Juan Channel sand wave field can be grouped into two classes based on size and shape. Nearly symmetric smaller sand waves were found toward the shallower parts of the wavefield in the north. These sand waves (zone 1 and 2) appear sharp and well defined with slightly steeper flanks facing north. The sand wave heights were 1–2 m, and wavelengths 30–40 m. The sand waves in the southern deeper section of the wavefield (zones 3 and 4) were larger and appeared more irregular. Smaller sand waves and mega-ripples were superimposed upon the large sand waves and fringe the sharp edges of the field. Two major crest orientations were detected, one with an East-

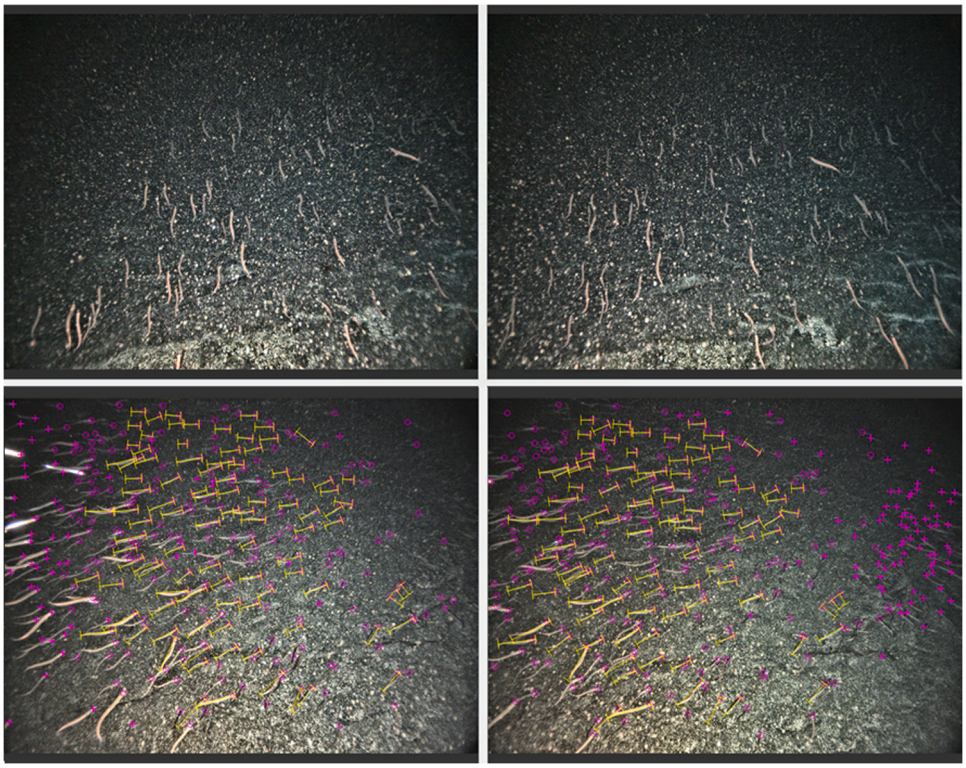

**Fig. 4.** Paired stereo-camera images were analyzed using SEBASTES open-source software (top figures). In post analysis (bottom figures), fish counts were analyzed by selecting points on the image where the eye of the fish could be seen in each frame (○). PSL that could not be seen in each image were still selected (+). PSL that were identified in each image pair and were positioned in a straight line were then measured (|——|).

West orientation (280°) and another with a Northwest–Southeast direction (315°). A Castaway CTD array collected temperature (°C) and salinity (PSU) profiles for submersible dives (Appendix, Fig. A-3a,c: submersible dive 1; Appendix Fig. A-3b,d; submersible dive 2). During the initial descent, the salinity probe provided erratic data. Otherwise, in both dives, temperature and salinity were relatively static (Appendix, Fig. A-3). In dive 1, temperature decreased and salinity increased as the submersible transited south and to greater depths, and then reversed as the submersible transited back north. This trend (i.e., decreased temperature and increased salinity at depth) was more prominent in the second dive, where the submersible transited nearly continuously south from a bottom depth of 40 m to a bottom depth of 80 m. On several occasions at various depths, the submersible was halted and lights turned off to detect ambient light conditions. Visible light was at a sufficient level to allow for human sight at most depths (40−70 m), but not at the greatest depths of the wavefield (70−80 m).

### 3.3. Fish abundance

A total of 313 (Dive 1 = 189; Dive 2 = 124) image pairs were analyzed for fish counts to determine maximum number of fish viewable in a single frame (MaxN). In Dive 1, 1691 PSL were observed, with a MaxN of 124 PSL (Fig. 5, left panel). A total of 6148 PSL were observed in Dive 2, with a MaxN of 409 PSL (Fig. 5, right panel; Table 1). A total of 402 PSL were sampled via Van Veen grab, with a maximum number of 49 fish per grab (Table 1).

### 3.4. Fish length

Fish length was analyzed by examining stereo-camera image pairs in partially automated image software (SEBASTES) and subsequently compared to fish lengths measured in the lab from samples collected in the field from Van Veen grabs. Lengths estimated from Dive 1 (Mean = 9.08 ± 2.86 mm, Range = 1.68−19.85 mm, N = 296) and Dive 2 (Mean = 8.90 ± 2.94 mm, Range = 1.42–19.92 mm, N = 810) were not significantly different (ANOVA: $F_{1,1104} = 2.21$, $P = 0.111$; Fig. 6, left panel). Moreover, length estimates in the submersible dives, analyzed using SEBASTES open source software were not significantly different from lengths measured from euthanized physical specimens measured in the laboratory sampled via Van Veen Grabs (Mean = 9.16 ± 1.1 mm, Range = 6.4–12.8 mm, N = 402; ANOVA, $F_{2,1506} = 2.94$, $P = 0.053$; Appendix, Fig. A-4). Length frequency histograms indicated similar distributions in lengths, though stereo-camera length estimates exhibited higher variance and range with some extreme measurements (Appendix, Fig. A-4), particularly on the upper end of the distribution (Fig. 6, center panel and right panel; Table 1).

### 3.5. Analysis of fish length and abundance in sections of the sand wave field

To determine whether fish abundance and/or fish length correlated with particular areas or morphologies of the sand wavefield, comparisons were made between (1) identified bathymetric zones of distinct wave period and amplitude, (2) North/South comparisons reflecting different depth ranges, and (3) differences in the center relative to the edge of the wave field. Significant differences in fish abundance were associated with distinct bathymetric zones in both Dive 1 (ANOVA: $F_{3,1695} = 8.70$, $P < 0.001$) and Dive 2 (ANOVA: $F_{2,970} = 16.84$, $P < 0.001$). Significant differences in abundance were also noted between the North and South sections of the wavefield (t-test: $t_{1,2670} = 12.02$, $P = 0.001$) and in subsection of the center-edge transect (ANOVA: $F_{19,221} = 5.52$, $P < 0.001$; Appendix, Fig. A-5a, Table 4). These differences, however, were largely driven by the emergence and dispersal of large numbers of fish, as indicted in analyses of the number of fish per frame (Appendix, Fig. A-6), rather than inherent differences in these habitat attributes. Comparisons of mean length (ANOVA: $F_{1,1065} = 0.81$, $P =$

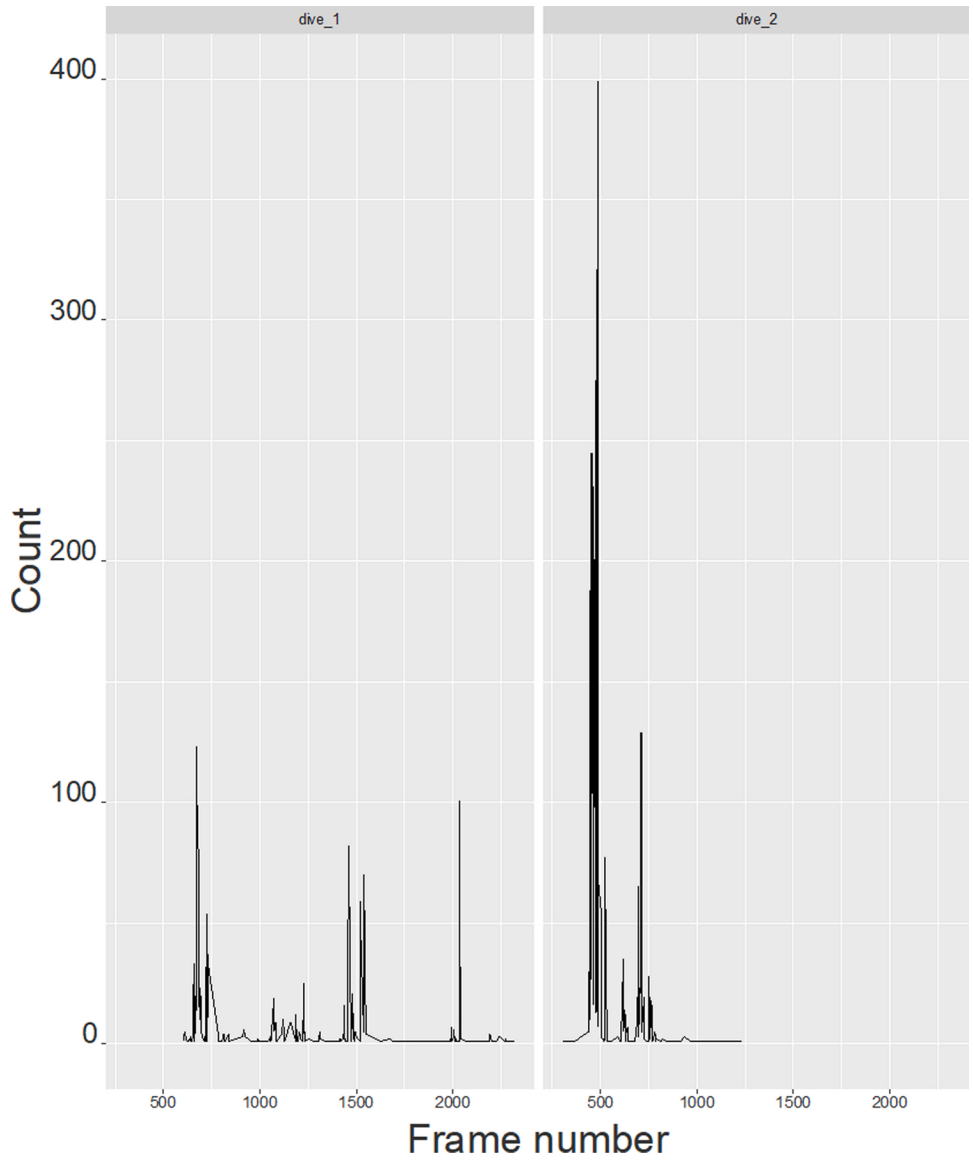


**Fig. 5.** Pacific sand lance counts per consecutive stereo-camera frame number during submersible dive 1 (maximum, N = 124) and dive 2 (maximum, N = 409).

**Table 1**
Sampling events at SJC sand wave field with surface Van Veen grabs and stereo-camera images secured through submersible Cyclops I submersible dives.

| Sampling approach | Year | Sampling Events | Start Time (GMT) | Start Time (GMT) | Duration (min) | Total fish observed | Fish per Van Veen | Fish per Image | Mean length ± SD (cm) |
|---|---|---|---|---|---|---|---|---|---|
| Van Veen | 2018 | 8 | – | – | – | 402 | 5.75 ± 8.26 | – | 9.16 ± 1.06, Range = 6.40–12.80, N = 402 |
| Dive 1 | 2018 | 1 | 17:20 | 20:20 | 180 | 1691 | – | 1.11 ± 7.5 | 9.08 ± 2.86, Range = 1.68–19.85, N = 296 |
| Dive 2 | 2018 | 1 | 19:54 | 21:34 | 100 | 6148 | – | 6.62 ± 33.35 | 8.90 ± 2.94, Range = 1.42–19.92, N = 810 |

*Notes*: Stereo-camera deployments at the San Juan Channel offshore wave fields through submersible dives were conducted in September 2018. Sampling with Van Veen grabs (N = 67 grabs) occurred on 8 sampling dates between September 15 and December 2. Note that stereo-camera length estimates <5 cm and >20 cm were not included in calculations, as there were assumed to be estimation errors.

0.368) in North and South sections of the wave field were not significantly different (Appendix, Fig. A-7; Table 2). Significant differences in mean fish length (ANOVA: $F_{3,1141} = 3.47$, $P = 0.016$) were detected between bathymetric zones of distinct wave period and amplitude (Fig. 7, Table 3, statistical tests compared zones 1–4, excluding zone 5 due to a low sample size). Tukey HSD pair-wise comparisons of individual zones noted significant distinctions in mean length between zones 1 and 4, such that fish in zone 1 were larger; no other between-zone distinctions were noted ($P > 0.351$). An analysis of a transect subsection from the center of the sand wave field to the edge (Appendix, Fig. A-2) failed to identify significant differences across the 20 subsections of this center-to-edge transect in mean length (ANOVA: $F_{19,\ 221`} = 0.57$, $P = 0.849$; Appendix, Fig. A-5b, Table 4).

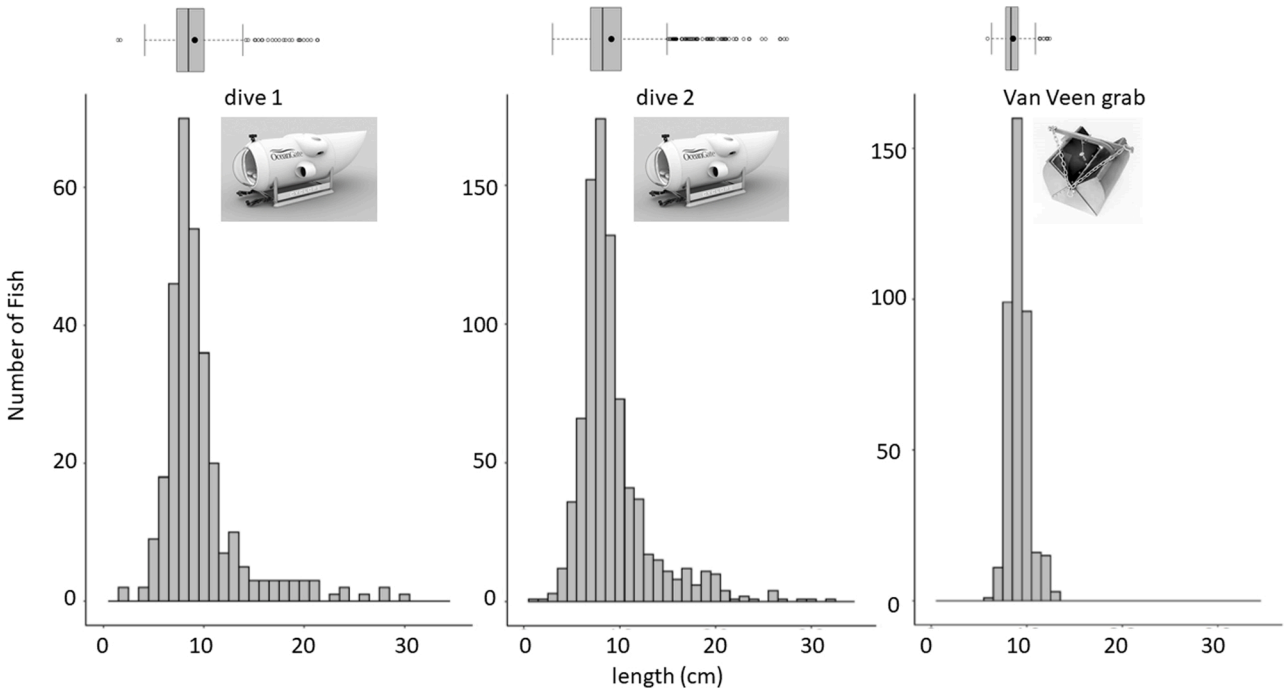


**Fig. 6.** Histograms and boxplots of total length of Pacific sand lance collected from the stereo-camera equipped submersible dives and the Van Veen grab samples (boxplots: box = interquartile range; dot = mean, line = median; whiskers = 95 % CI; points = outliers).

**Table 2**
Fish abundance and fish length as a function of North and South sections of the SJC sand wave field (dives 1 and 2 combined).

| Area | Fish per Image frame | Mean length (cm) | Mean length (cm) |
|---|---|---|---|
| | | All values | Incidence Angle <°50 |
| North | 1.4 ± 8.49, Range = 0–124 | 9.29 ± 2.92, Range = 5.05–19.01, N = 197 | 7.95 ± 1.65, Range = 1.68–13.90, N = 139 |
| South | 4.19 ± 26.81, Range = 0–400 | 9.08 ± 2.86, Range = 1.68–19.85, N=909 | 7.73 ± 1.69, Range = 1.42–16.64, N = 524 |

### 3.6. Analysis of fish length, proclivity to school, and position within the school

To determine whether or not fishes aggregated according to size or whether fish size dictated position within a school, analyses were conducted on (1) the relationship between mean length and the number of fish within the school; and (2) the relationship between mean length and the distance from the center of the school. While no significant relationship was noted related to mean length and number of fish within a school ($R^2 = 0.02$, $P = 0.357$), the largest schools (N > 100) were comprised of mostly smaller fish and larger fish were more frequently observed in isolation or in small numbers (Appendix, Fig. A-8a). While not significant, a weak trend was observed in the relationship between fish size and position within the school (i.e., distance from center of the school), suggesting that larger fish might be more frequently associated with the edge of the school ($R^2 = 0.10$, $P = 0.080$; Appendix, Fig. A-8b).

### 3.7. Analysis of error associated with stereo-camera measurements

Stereo-camera derived maximum volumetric density of PSL peaked at 378 fish/m$^3$ at a range of 1.125 m from the camera and mean volumetric density of PSL peaked at 24.5 fish/m$^3$ at a range of 1.375 m from the camera (Fig. 8). Lower volumetric fish densities in the near-field were clearly evident and likely a result of fish avoidance of the submersible, while the ability to detect PSL decreased as a function of distance from camera, particularly as it extended beyond the observed peak density range. An analysis of length estimates as a function of fish angle relative to the camera showed that fish lengths tended to be overestimated at the greatest distances from the camera and at the periphery of the image space (Fig. 9a). Moreover, length estimates were more variable when fish were > 50° from orthogonal to the camera viewing direction (Fig. 9b). An analysis of the variance in length as a function of incidence angle showed that variability increased rapidly beyond the > 50° threshold (Fig. A-9). Regression analysis applied to the standard deviation of length measurements for 5-degree bins identified a breakpoint at 50°; the best least squares fit was achieved when adopting a piece-wise approach, using a two-segment regression with the breakpoint at 50°. This steep increase in error (i.e., increase in standard deviation in length measurement) as a function of incidence angle > 50° is shown in supplementary materials (Appendix, Fig. A-9). To further explore the error associated with these results, fish > 50° from orthogonal to the camera were subsequently excluded from length measurements and related analyses. Following the removal of high incidence angle fish, variation in fish length as a function of range (e.g., distance from the camera) was reduced by an order of magnitude ($R^2 = 0.01$, $P = 0.004$, N = 664; Fig. 9c, black lines), in comparison to variation in length measurements with the full data ($R^2 = 0.11$, $P < 0.001$, N = 1145; Fig. 9c, blue lines).

### 3.8. Revised analyses with correction factor for incidence angle

There were 664 fish measured where the incidence angle was < 50°. In a revised analysis including only these fish, trends evident in the initial analyses were maintained. Fish lengths obtained from Dive 1 (Mean = 8.00 ± 1.63, Range = 1.68–13.90, N = 145) and Dive 2 (Mean = 7.72 ± 1.70, Range = 1.42–16.64, N = 518) still showed no significant difference (ANOVA: $F_{1,662} = 3.16$, $P = 0.076$). Fish lengths in the four distinct bathymetric zones still indicated significant differences in mean length (ANOVA: $F_{3,659} = 3.69$, $P = 0.012$) and Tukey HSD pair-wise comparisons distinguished mean lengths in zone 1 and 4 ($P < 0.044$), but in no other pairwise comparisons ($P > 0.169$). Comparisons of mean length in North and South sections of the wave field remained statistically indistinguishable (ANOVA: $F_{1,661} = 1.75$, $P = 0.186$). No

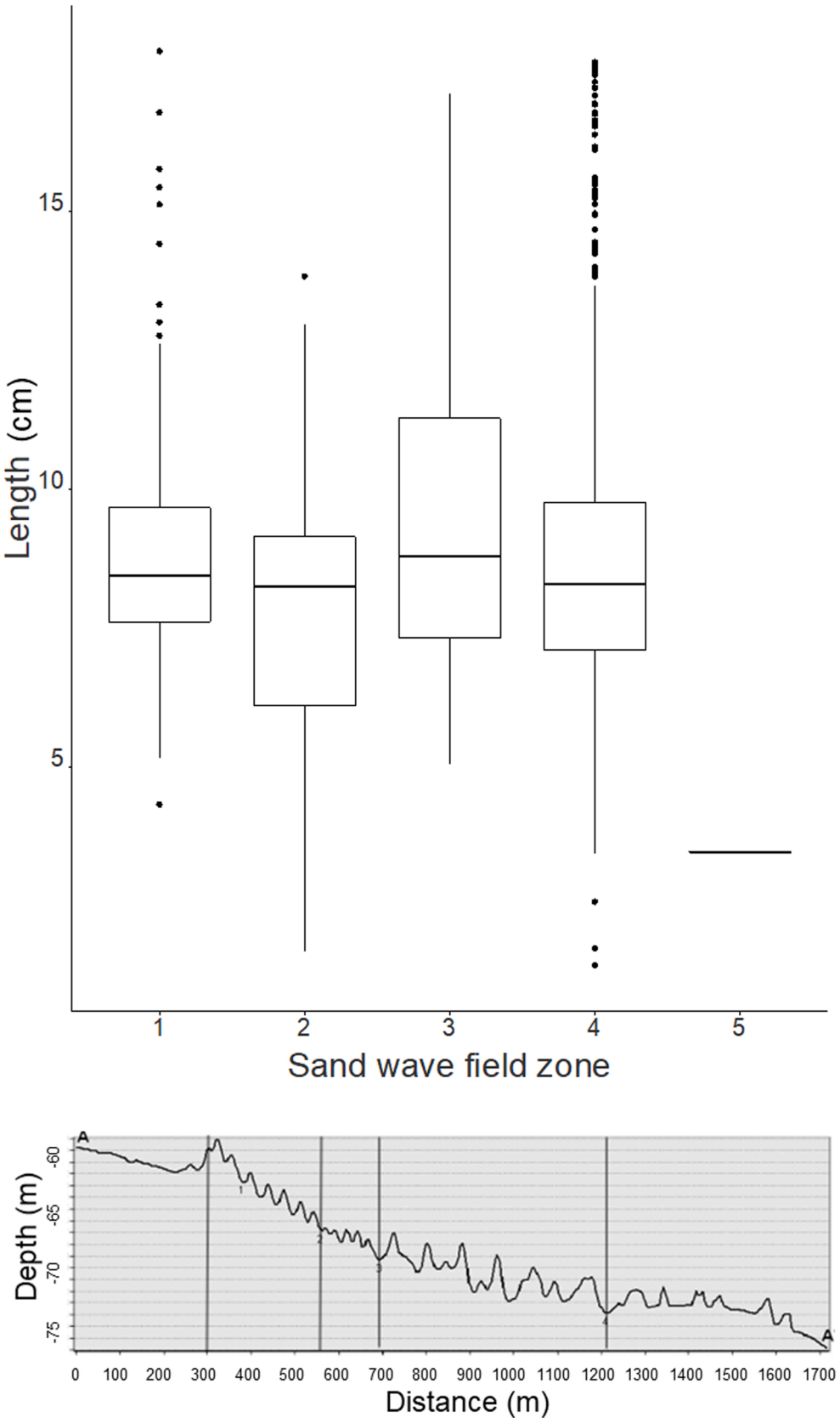


**Fig. 7.** Lower panel: Identified subsections of the SJC wave field as per Greene et al., 2017, from north (A) to south (A´). Upper panel: Box plots of total length of schooling Pacific sand lance observed within discrete identified sections of the SJC sand wave field, data from both dives combined (box: interquartile range; line: median; whiskers: 95 % CI; points: outliers).

**Table 3**
Fish abundance and fish length as a function of distinct bathymetric sections of the SJC sand wave field related to wave period and amplitude (dives 1 and 2 combined).

| Area | Fish per Image frame | Total Fish | Mean length (cm) All values | Mean length (cm) Incidence Angle <°50 |
|---|---|---|---|---|
| Zone 1 | 2.18 ± 11.29, Range = 0–124 | 850 | 9.47 ± 4.00, Range = 4.32–23.42, N = 118 | 8.36 ± 1.48, Range = 4.32–12.61, N = 56 |
| Zone 2 | 0.55 ± 2.41, Range = 0–25 | 194 | 8.63 ± 4.37, Range = 1.68–23.52, N = 30 | 6.88 ± 2.14, Range = 1.68–9.98, N = 14 |
| Zone 3 | 1.4 ± 8.79, Range = 0–101 | 363 | 9.94 ± 3.56, Range = 5.05–20.21, N=94 | 7.83 ± 1.58, Range = 5.05–13.90, N = 69 |
| Zone 4 | 5.69 ± 31.12, Range = 0–400 | 6415 | 9.15 ± 3.33, Range = 1.42–24.20, N=908 | 7.74 ± 1.69, Range = 1.42–16.64, N = 523 |
| Zone 5 | 0.02 ± 0.2, Range = 0–3 | 9 | 3.46 ± NA, Range = NA, N = 1 | 3.46 ± NA, Range = NA, N = 1 |

significant differences were noted between the 20 subsections of the transect from center to edge of the sand wavefield overall (ANOVA: $F_{9,64} = 1.01$, $P = 0.449$). Direct comparison of individual center-to-edge transect subsections demonstrated that individual subsections did not differ from one another (Tukey HSD hoc tests, $P > 0.557$; Table 4). The re-analysis of data without high incidence angle (> 50°) fish also determined that there was no trend in fish length as a function of fish position within the school (distance from center; $R^2 = 0.04$, $P = 0.294$).

### 3.9. Fish behavior and response

Fish response to submersible activity was evident in preliminary observations within the submersible, as well as in subsequent analyses of the data (Fig. 10). Several observations were immediately evident. Fish responded to physical disturbance to the sand wavefield and emerged immediately following contact with the benthos. Peaks of abundance observed throughout the dives coincided with bottom contact for the submersible and these events were followed by reburial or disaggregated and erratic behavior by the fish, subsequently followed by organized schooling dynamics, and subsequently burying behavior. Fish were generally not visible or active during periods of stationary observation, regardless of whether the lights of the submersible were on (Fig. 10). In general, once disturbed and in the water column, fish were attracted to the submersible lights. While natural light at bottom was limited, deliberate black-out intervals of observation allowed our eyes to adjust to ambient light in natural conditions. Analysis of accompanying video footage of the dives suggested that the pulsed strobe light associated with the stereo-camera array had no perceivable effect on fish behavior.

## 4. Discussion

### 4.1. Value of observational data in submersible surveys

These submersible surveys enabled observations of PSL *in situ* that provided insights into pelagic schooling dynamics, entry and exit from benthic sediments, interactions with currents, sand wave morphology, light, and disturbance. It also enabled visual surveys of the full extent of an important benthic habitat. This served to groundtruth observations and inferences previously made from MBES bathymetry and soundings. While past research had focused on Van Veen grab sampling for fish and sediment samples, viewing PSL in their natural environment answered important questions on light penetration and response to disturbance. It also raised new questions about schooling dynamics, aggregation and dispersal, evasion and attraction, predation, and response to tidal, diel,

**Table 4**
Fish abundance and fish length (mean, SD) as a function of a subsection of the transect from center to edge within the SJC sand wave field.

| Minutes from Center of SJC sand wavefield | Fish per Image frame | Total Fish | Depth (m) | Mean length (cm) All values | Mean length (cm) Incidence Angle <°50 |
|---|---|---|---|---|---|
| Minute 1 | 0.08 | 1 | 70–72 | – | – |
| Minute 2 | – | – | 70–72 | – | – |
| Minute 3 | 1.50 | 18 | 71–73 | 8.46 ± 5.33 Range = 1.73–13.92, N = 5 | – |
| Minute 4 | 10.23 | 133 | 70–72 | 9.13 ± 3.00 Range = 5.02–21.20, N = 33 | 7.92 ± 1.32, Range = 5.02–10.09, N = 24 |
| Minute 5 | 30.83 | 370 | 71–73 | 8.78 ± 3.10 Range = 3.53–19.92, N = 49 | 7.62 ± 1.93, Range = 3.53–12.16, N = 29 |
| Minute 6 | 1.58 | 19 | 72–74 | 9.85 ± 3.55 Range = 7.06–17.08, N=7 | 8.13 ± 1.32, Range = 7.06–10.37, N = 5 |
| Minute 7 | 0.18 | 2 | 72–74 | 9.67 ± 3.86 Range = 6.94–12.40, N = 22 | 6.94 ± NA, Range = NA, N = 1 |
| Minute 8 | 0.50 | 6 | 73–75 | 6.49 ± 2.24 Range = 4.10–19.85, N = 3 | 6.49 ± 2.24, Range = 4.10–8.53, N = 3 |
| Minute 9 | 2.83 | 34 | 72–74 | 10.07 ± 4.12 Range = 6.64–19.85, N=6 | 7.04 ± 0.36, Range = 6.64–7.34, N = 3 |
| Minute 10 | 3.58 | 43 | 73–75 | 9.59 ± 3.83 Range = 5.99–17.23, N=8 | 8.48 ± 2.44, Range = 5.99–10.87, N = 4 |
| Minute 11 | 1.64 | 18 | 74–76 | 10.07 ± 3.13 Range = 4.90–15.48, N = 10 | 9.42 ± 0.78, Range = 8.61–10.17, N = 3 |
| Minute 12 | 0.50 | 6 | 73–75 | 8.80 ± NA Range = NA, N = 1 | 8.8 ± NA, Range = NA, N = 1 |
| Minute 13 | – | – | 74–76 | – | – |
| Minute 14 | 0.25 | 3 | 72–74 | 11.03 ± NA Range = NA, N = 1 | – |
| Minute 15 | – | – | 72–74 | – | – |
| Minute 16 | 0.08 | 1 | 70–72 | 10.15 ± NA Range = NA, N = 1 | 10.15 ± NA, Range = NA, N = 1 |
| Minute 17 | – | – | 70–72 | – | – |
| Minute 18 | – | – | 70–72 | – | – |
| Minute 19 | – | – | 70–72 | – | – |
| Minute 20 | – | – | 70–72 | – | – |

and seasonal drivers. It will be critical to further investigate how patterns in light, tidal currents, and seasonal production influence patterns in foraging in the water column and dormancy in sediments, patterns known to be influenced by both diel (Baker et al., 2021a, in prep.) and seasonal timeframes (Baker et al., 2019b).

#### 4.1.1. Improved understanding of benthic habitat, substrates, conditions, and currents

The SJC sediment wavefield represents an extensive sub-tidal habitat feature, important to PSL (Greene et al., 2020). The bathymetry throughout much of the eastern North Pacific and Gulf of Alaska includes deep straits and channels carved out by glaciers with significant

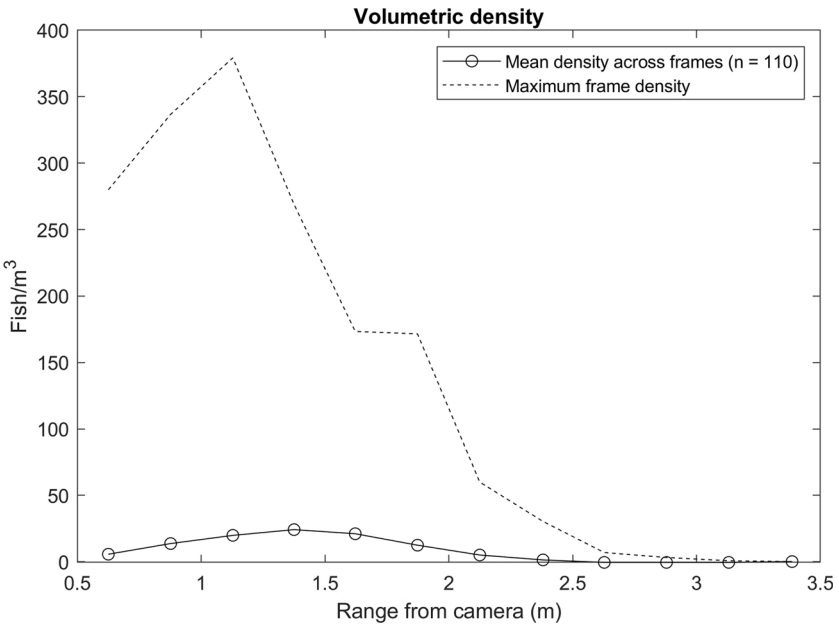


**Fig. 8.** Volumetric density of fish (fish/$m^3$), measured as a function of the range from the camera (m). Mean density across all frames (–○–) is contrasted to maximum recorded frame density (– –). Volumetric fish density analysis using the estimated camera viewing volumes and the 3-dimensional position of fish targets shows a clear near-field avoidance effect.

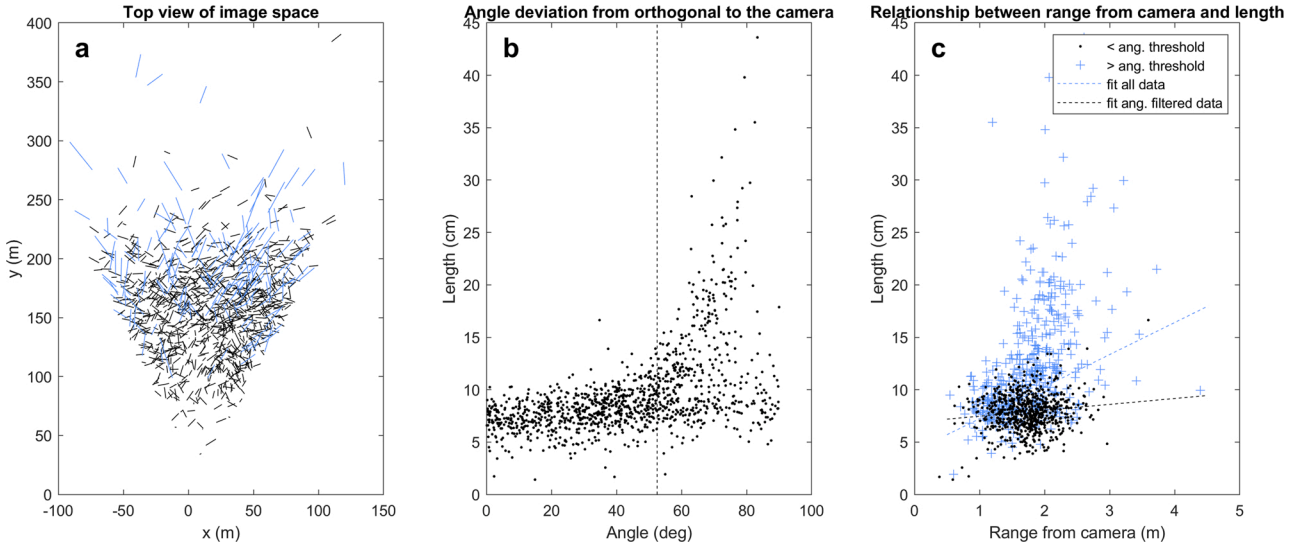


**Fig. 9.** Measurement error for fish lengths as a function of distance from the camera and angle deviation from orthogonal position. A top view of the image space (a) demonstrates that error for fish estimated at lengths beyond observed measurements in captured specimens (>12 cm) was typically at the greatest distances from the camera (extreme y-axis values) and at the periphery of the image space (extreme x-axis values). The relationship of estimated fish length as a function of range from the camera (b) is shown as a function of the linear distance from target. Fish position or angle deviation from orthogonal to the camera (c) added error to length estimates. Fish lengths tended to be overestimated when fish were > 50° from orthogonal to the camera. The removal of fish > 50° from orthogonal not only removed extreme values for length measurements, but removed the effect of distance from camera.

sediment deposits and strong tidal exchange with strong currents (Zimmermann et al., 2019; Ormseth et al., 2019). Similar features to the SJC sand wavefield have been found throughout this region (Barrie et al., 2009), including elsewhere in the San Juan Archipelago (Greene and Barrie, 2011). Though limited in area and extent, these benthic features consist of low silt, relatively well-sorted coarse sand to fine gravel sediments, and may provide important habitat for winter dormancy. Understanding complex benthic substructure such as this one may be important to understanding fish-habitat relationships in PSL. Differences in topographic complexity have been linked to spatial variability in the abundance and distribution of other forage fishes. Potential differences in oceanographic properties driven by currents, flow, and complex bathymetry may influence distribution for a wide variety of pelagic species (McGowan et al., 2019). The use of inshore habitats by fishes in the Gulf of Alaska (Ormseth et al., 2017) and California Current (Yoklavich et al., 1991; Muhling et al., 2019) has been shown to be extensive. Moreover, these inshore habitats are not only important to forage fishes, many fishes inhabit inshore areas as juveniles. Quantifying habitat use in these areas may be critical to informing life history and to understanding recruitment in fish populations more generally.

These submersible surveys provided important confirmation of data

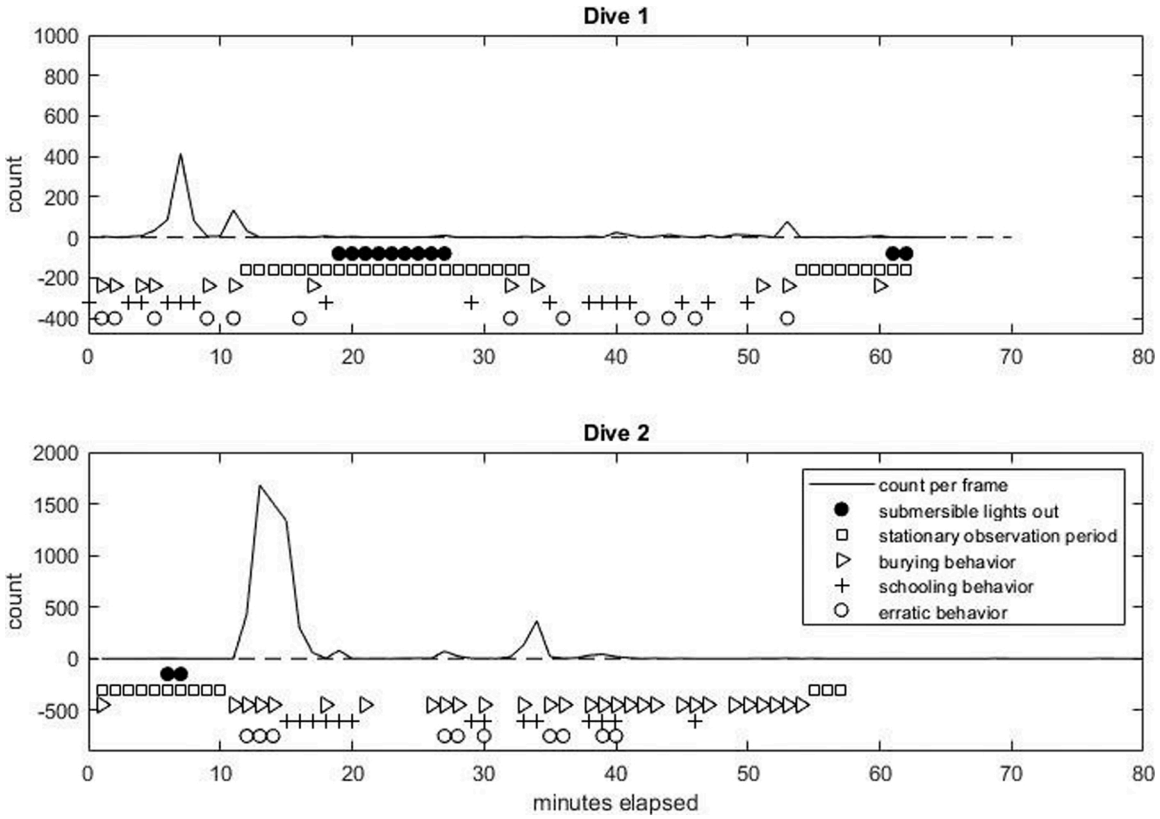


**Fig. 10.** Sequence of fish observations in dive 1 (top plot) and dive 2 (bottom plot). Submersible operations that deviate from standard operation with movement and operational lights are indicated for stationary observation periods (□) and stationary observation periods without operational lights (●). Fish count per frame is indicated (—) and observed fish behavior is indicated in the form of three behavioral modes, including active schooling or shoaling (+), burying (▶), or erratic/uncoordinated movements (○).

recorded through alternate methods (e.g., acoustic Doppler current profile systems, Greene et al., 2017; sediment processing, Baker et al., 2021b, In Review). It also provided further support for the importance of tidal currents and flow in shaping and maintaining this dynamic bedform habitat (Greene et al., 2017) and confirmed prominent physical attributes of this habitat, related to wave height, periodicity and substrate composition and deposition. Submersible observations provided insight on important environmental attributes, such as light penetration. Despite the significant depth (60−80 m), ambient light was sufficient for us to perceive the surrounding area. Given that PSL are adapted to extremely low light conditions relative to other North Pacific fishes (Britt et al., 2001), it is evident that this light is sufficient to relay information on diel cycles. The fish (*Ammodytes* spp.) are responsive to light (Winslade, 1974) and have been observed to exhibit diurnal patterns in foraging (Hobson, 1986; Freeman et al., 2004; Baker et al., 2021a, In Prep.) and seasonal shifts in activity relative to daylight duration (e.g., winter dormancy, winter spawning, and spring emergence; Robards et al., 1999; van Deurs et al., 2010). Other studies have demonstrated that *Ammodytes* spp. may also be able to perceive light levels through sediments and receive these cues while buried and dormant; thus light may be a limiting factor in benthic habitat selection. Ostrand et al. (2005) demonstrated a strong selection for shallow water through habitat selection models and suggested that limits to light penetration at depth may be a limiting factor for habitat use. Our observations at 60−80 m, suggest light may not be a limiting factor at these depths. While it is expected that there is a high degree of variability in light conditions, observations occurred in September (approximately equinox) in both clear and overcast conditions and therefore may serve as a useful proxy for conditions in other seasons. This observation, though essentially a one-time observation, is instructive and provides a rationale for more intensive and precise measurements through traditional methods (e.g., using light meters at various deep-water locations known to support this species). This might be used to measure Lux at depth at seasonal intervals and in varied conditions to understand light penetration as a function of photoperiod, calendar date, and relative production or turbidity in the water column

#### 4.1.2. *Improved understanding of Pacific sand lance dynamics and response*

Submersible dives allowed direct access to the natural habitat for this species. That enabled insights on behavioral attributes, schooling dynamics, and response to disturbance. Most evidently in our surveys, contact with the seafloor caused disturbance to bottom substrates and related shock waves that precipitated rapid expulsion of PSL from the surrounding sediments. Also, proximity to the bottom and the related pressure wave and noise of the submersible appeared to flush fish from the sediments. These observations not only provide insights related to potential biases in the use of vehicles and disturbance in observing and estimating fish, but also related to potential predation on PSL within bottom sediments and escape response mechanisms. It appears that fish may respond to disturbance with an immediate escape response, followed by a disaggregated and disorganized response. Following this, fish appear to either rebury or reorient to school in an organized formation. Submersible observations also provided some insight into swimming dynamics. As documented in a similar species *(Ammodytes marinus*; Kubilius and Ona, 2012) fish seemed to swim with a positive tilt. More research is needed to quantify these attributes, but this seems to reflect the fact that sand eels and sand lance lack a swim bladder and are negatively buoyant. To maintain altitude, these fish must swim with some positive body tilt such that a positive lift is generated at slow swimming speed by moving with a head-up posture. This also suggests that PSL may tend to stay and forage within a small local area. This is

supported by multiple studies of *Ammodytes* spp. that suggest these fish forage in close proximity (<5 km) to resident sediments (*Ammodytes marinus*: Wright et al., 2000; van der Kooij et al., 2008; *Ammodytes hexapterus*: Tokranov, 2007) and extensively re-use sediments and demonstrate site fidelity (*Ammodyes personatus:* Haynes and Robinson, 2011).

#### 4.1.3. Potential biases related to submersible surveys

It is well known that vehicles used in surveys (including submersibles) may bias observations through disturbance and fish attraction or avoidance responses. Resulting abundance estimates may therefore be strongly influenced by species and size-specific fish behavior (Trenkel et al., 2004; Williams et al., 2014; McIntyre et al., 2015). Fish avoidance or attraction to surface vessels (De Robertis and Handegard, 2013) or submersibles (Stoner et al., 2008) has been shown to occur and these responses have been demonstrated to bias survey density estimates (Koslow et al., 1995; Yoklavich et al., 2007). This disturbance may occur in multiple ways. There may be reactions to the optical platform itself, especially for moving platforms such as remotely operated vehicles (ROV) and drop cameras. Fish may experience both auditory and visual stimuli prior to the passage of the observing vehicle with response at both the individual (e.g., position, speed, direction) and group (e.g., spacing, alignment, aggregation) level (Laidig et al., 2013; Somerton et al., 2017). Rockfishes (*Sebastes* spp.) have been observed to exhibit an escape response to underwater vehicles (Krieger et al., 2001; Stoner et al., 2008; Rooper et al., 2020). This response may be species- and/or size-specific. In our surveys artificial lighting was also required to navigate and observe fish. In most deep-water marine environments, artificial lighting is necessary for optical surveys, and the reactions of fish to the intensity and type of lighting is also poorly understood (Ryer et al., 2009; Rooper et al., 2015). Moreover in this species, bottom contact caused the emergence of fish from sediment. Disturbance to habitat is a critical consideration for the use of submersibles for any fish that actively uses habitat for refuge or cover.

### 4.2. Application of stereo-camera to fisheries surveys

Underwater stereo-cameras provide an efficient and alternative method to observe and measure fish in areas that are difficult to sample (Rooper et al., 2010; Williams et al., 2010) and have increasingly been used to sample pelagic fish populations (Boldt et al., 2018). Stereo-camera images enabled quantified calculations on PSL that were observed *in situ.* Evidence for preferences for particular areas within the SJC sand wavefield were inconclusive for population-wide preference. No zone-specific length differences were observed in any location grouping (NS, Zones 1–5, Center-Edge transect), despite large sample sizes. This may be a reflection of largely uniform physical attributes throughout this benthic habitat feature. Both fish counts and distribution were highly variable within dives. This appears to largely be a reflection of submersible-related disturbance. Additional survey work would be required to adequately quantify abundance through this approach. Additionally, methodology would need to be further standardized to account or at least control for disturbance effects (e.g., benthic agitation and disturbance). Furthermore, seasonal and diel effects and conditions related to tidal effects or turbulence might significantly influence abundance estimates. We concluded that PSL do not have size-specific preferences related to wave height or length, or distance from the center of the wave field. Given these observations, it seems unlikely that PSL habitat preference is based on the physical characteristics and variability examined here. It is more likely related to bedform physical characteristics like sediment uniformity, grain size, and oxygen content that, in this instance, were relatively uniform across the surveyed area. Van Veen grab data, which samples a standardized volumetric area of sediment, is less likely to be biased by disturbance effects and may serve as a better source of information for relative fish abundance and fish distribution within habitats. Still, observational data via submersible surveys may inform potential sampling bias inherent in alternative methods (e.g., trawls, grabs, acoustics), by understanding fish behavior within the water column, movement between pelagic and benthic habitats, and proximity to bottom. Submersible surveys may also provide a more efficient approach to data collection (e.g., an efficient alternative to length estimation). These methodologies are significantly different in their approach and strengths.

#### 4.2.1. Complement and contrast to alternative methods

Used either in isolation or in combination with other approaches, stereo-camera data may provide a useful contrast to inform potential biases to alternate methods (van Duers et al., 2012; Freeman et al., 2004) and provide a unique perspective, particularly on species difficult to assess through alternative methods. Cameras can also sample in areas where trawling is not possible (e.g., shipping lanes), or permitted (e.g., marine protected areas). The use of the stereo-camera in unison with submersible transects allowed us to further investigate submersible observations and quantify responses and metrics. Stereo-cameras can also serve as viable tools for acoustic target verification of fish species and measurements of fish lengths. Additional information on specific fish depth, tilt, and yaw may also be calculated, which provide further insights into fish orientation and schooling.

#### 4.2.2. Potential biases and approaches to improve estimates of morphological measurements

The stereo image analysis process can introduce biases in measurements due to imperfect calibrations and variability in user-specified fish end points on images. In this study, mean length measurements estimated from the stereo-camera closely replicated estimates from physical specimens measured in the lab. Despite that, the variance in stereo-camera fish length measurements at the extremes was pronounced. Our results showed definitively that errors in length measurements were amplified when fish orientation was $> 50^{\circ}$ from orthogonal to the camera viewing direction. Following exclusion of data influenced by incidence angle, the application of standardized built-in stereo-imaging methods in SEBASTES software appear to otherwise compensate for changes in fish appearance as a function of distance from the camera. Similar analyses have also noted differences in error related to fish orientation. Boldt et al. (2018) reported that fish length measurements were most accurate when yaw angles were $< 30^{\circ}$. While removing measurements with higher angles relative to the camera substantially reduced the overall number of possible measurements that could be made, the randomized nature of fish orientation relative to the camera reduces the possibility that some size classes were less available to be measured by the camera.

Volumetric fish density analysis using the estimated camera viewing volumes and the 3D position of fish targets also showed a clear near-field avoidance effect. This was in part due to the location of the camera platform, which was approximately 0.5 m behind the forward-most point of the submersible. Observations of fish school movement also indicated fish attraction to the submersible lighting, which would indicate that the densities observed by the camera may not represent true undisturbed fish densities. These areas of potential bias need further investigation and would need to be resolved prior any standardized use of submersibles to estimate abundance. Use of submersibles with direct human observation in situ, while often prohibitively expensive, may provide useful insights into what factors deserve further investigation and how to implement controls.

#### 4.2.3. Potential biases and approaches to improve estimates of abundance

Our results support past evidence (Williams et al., 2010) that stereo-based optical sampling is a viable method for augmenting alternate forms of abundance estimations. Stereo-cameras allow quantitative surveys of abundance and can also be used to observe and quantify the behavior of fish. Standard approaches use MaxN as a conservative count of fishes (Denney et al., 2017). MaxN is the maximum number of fish

observed within a single frame, used to avoid double counting fish that leave and return to a frame. Our abundance estimates using MaxN therefore serves as a minimum number of fish present and may underestimate true fish abundance. While this is an important consideration, biases to abundance estimates are expected in pelagic fishes and may be best ameliorated through adopting an absolute density approach, where each frame can be considered as a measure of fish density in either volumetric or areal terms (Williams et al., 2018).

### 4.3. Future applications

This study effectively applied submersible observation and stereo-camera image analysis as an alternate sampling methodology to examine relationships between PSL and sand wavefield attributes. The use of these methodologies may complement other sampling approaches and, in this instance, furthered understanding of this forage fish and its use of benthic habitat. Future studies are intended to use stereo-cameras to assess PSL presence at other subtidal benthic habitats, as well as beach habitats. Further work also aims to documents diel vertical migration and analyzes fish movement and behavior patterns, disturbance events, schooling dynamics, and reactions to predators.

## Supplemental information

Additional information on this research effort is available through OceanGate. https://oceangate.com/expeditions/salish-sea-survey-expedition.html and the SeaDoc Society https://www.seadocsociety.org/submersible. Additional videos are available at the following links: https://youtu.be/wsEnDkoPFS8; https://youtu.be/h-UdTQsvIYc.

## CRediT authorship contribution statement

**M.R. Baker:** supervision, conceptualization, methodology, data analysis, visualization, writing. **K. Williams:** conceptualization, methodology, data analysis, visualization, writing, technical support. **H.G. Greene:** supervision, conceptualization, methodology, writing. **C. Greufe:** data analysis, visualization. **H. Lopes:** data analysis, visualization. **J. Aschoff:** visualization. **R. Towler:** technical support.

## Declaration of Competing Interest

The authors report no declarations of interest.

## Acknowledgments

We greatly appreciate the efforts of Joe Gaydos and the SeaDoc Society, Orcas Island, WA to secure and facilitate the use of the OceanGate Cyclops I to conduct these underwater observations. We also greatly appreciate the work of OceanGate Inc. leadership and the OceanGate engineers, plan teams and dive teams to dedicate their time, personnel, and equipment to support this research, particularly Stockton Rush, Wendy Rush, Russell McDuff, Tony Nissen, Chris Howard, Neil McCurdy, and Mikayla Monroe. This research effort was also supported by the administration, staff, and boating team of the R/V Centennial and the University of Washington Friday Harbor Laboratories. We particularly appreciate the efforts of Megan Dethier, David Duggins, and Neil Smith. We also appreciate the support of the School of Oceanography and the School of Aquatic and Fishery Sciences, particularly Meegan Corcoran and Andre Punt. This research resulted from a collaboration with the Midwater Assessment and Conservation Engineering program at the NOAA Alaska Fisheries Science Center. Equipment was developed through the NOAA Advanced Sampling Technology Working group. We thank Chris Wilson and Chris Rooper for technical and logistical support. We also thank Sandy Parker-Stetter, Peter Frey, Tom Laidig, David Bryan and Lyle Britt for internal review and comments on this manuscript. This work builds on the efforts and insights of researchers at the Washington Department of Fish and Wildlife, particularly Bob Pacunski and his efforts to identify important habitats and advance the field of ROV research. We also recognize the importance of longterm monitoring and the annual research conducted through the Pelagic Ecosystem Function Research Apprenticeship at the University of Washington Friday Harbor Laboratories as well as the Mary Gates Research Endowment to support the involvement of students in the exploration and analysis of these data. Reference to trade names does not imply endorsement by the National Marine Fisheries Service, NOAA. The findings and conclusions in the paper are those of the authors and do not necessarily represent the views of the National Marine Fisheries Service, NOAA. Use of the Cyclops I submersible and logistical support for the dive effort was provided through the OceanGate Foundation and SeaDoc Society (Groundtruthing Pacific sand lance habitat characteristics and occurrence in a known deep water habitat – the San Juan Channel sand wave field, Central Salish Sea, Washington.

## Appendix A. Supplementary data

Supplementary material related to this article can be found, in the online version, at doi:https://doi.org/10.1016/j.fishres.2021.106067.

## References

Alheit, J., Peck, M.A., 2019. Drivers of dynamics of small pelagic fish resources: biology, management and human factors. Mar. Ecol. Prog. Ser. 617, 1–6.

Auster, P.J., Lindholm, J., Schaub, S., Funnell, G., Kaufman, L.S., Valentine, P.C., 2003. Use of sand wave habitats by silver hake. J. Fish Biol. 62 (1), 143–152.

Baker, M.R., 2021. Contrast of warm and cold phases in the Bering Sea to understand spatial distributions of Arctic and sub-Arctic gadids. Polar Biol. 44 (6), 1083–1105. https://doi.org/10.1007/s00300-021-02856-x.

Baker, M.R., Hollowed, A.B., 2014. Delineating ecological regions in marine systems: integrating physical structure and community composition to inform spatial management in the eastern Bering Sea. Deep. Sea Res. Part Ii Top. Stud. Oceanogr. 109, 215–240. https://doi.org/10.1016/j.dsr2.2014.03.001.

Baker, M.B., Siddon, E., Saitoh, S.I., Nishikawa, H., 2018. Influence of climate and environmental variability on pelagic and forage species. In: S11: MONITOR Topic Session. North Pacific Marine Science Organization, PICES Annual Science Conference. Yokahama, Japan. https://meetings.pices.int/meetings/annual/2018/pices/Program.

Baker, M.R., Palsson, W., Zimmermann, M., Rooper, C.N., 2019a. Model of trawlable area using benthic terrain and oceanographic variables—informing survey design and habitat maps in the Gulf of Alaska. Fish. Oceanogr. 28 (6), 629–657.

Baker, M.R., Matta, M.E., Beaulieu, M., Paris, N., Huber, S., Graham, O.J., Pham, T., Sisson, N.B., Heller, C.P., Witt, A., O'Neill, M.R., 2019b. Intra-seasonal and inter-annual patterns in the demographics of sand lance and response to environmental drivers in the North Pacific. Mar. Ecol. Prog. Ser. 617-618, 221–244.

Baker, M.R., Smeltz, T.S., Williams, K., Greufe, C., Chapman, J., Ewing, M., Glassy, J., Hasegawa, E., Cieri, K., Matson, S., Towler, R., 2021a. Diel vertical migration in a pelagic forage fish (*Ammodytes personatus)* associated with benthic substrates. In Prep Behav. Ecol.

Baker, M.R., Greene, H.G., Aschoff, J., Bates, E., Hoge, M., Aitoro, E., Childers, S., Johnson, K., Sealover, N., Tinnon, A., Bynum, K., Lopez, J., Thomson, A., 2021b. Analyses of sediment association and distribution of Pacific sand lance (*Ammodytes personatus*) in a benthic sand wave field. In Review Cont. Shelf Res.

Barrie, J.V., Conway, K.W., Picard, K., Greene, H.G., 2009. Large scale sedimentary bedforms and sediment dynamics on a glaciated tectonic continental shelf: examples from the Pacific margin of Canada. Cont. Shelf Res. 29, 796–806.

Bishop, J., 2006. Standardizing fishery-dependent catch and effort data in complex fisheries with technology change. Rev. Fish Biol. Fish. 16 (1), 21.

Bizzarro, J.J., Peterson, A.N., Blaine, J.M., Balaban, J.P., Greene, H.G., Summers, A.P., 2016. Burrowing behavior, habitat, and functional morphology of the Pacific sand lance (*Ammodytes personatus*). Fish. Bull. 114 (4).

Boldt, J.L., Baker, M.R., Bernal, M., Somarakis, S., Essington, T.E., 2017. Methods and techniques for sampling and assessing small pelagic fish populations. In: Jürgen Alheit (ICES) and Yoshioki Oozeki (PICES) ICES/PICES Symposium on Drivers of Dynamics of Small Pelagic Fish Resources. Victoria, Canada. https://meetings.pices.int/meetings/international/2017/pelagic/program#W2.

Boldt, J.L., Williams, K., Rooper, C.N., Towler, R.H., Gauthier, S., 2018. Development of stereo camera methodologies to improve pelagic fish biomass estimates and inform ecosystem management in marine waters. Fish. Res. 198, 66–77.

Boldt, J.L., Gauthier, S., King, S., Arimitsu, M., Baker, M.R., Sandell, T., Neville, C., Flostrand, L., Bertram, D., Perry, I., Tucker, S., Robinson, C., Melvin, G., Murphy, H., McQuinn, I., Majewski, A., Geoffroy, M., Debertin, A., Hipfner, M., Hunt, B., Menard, N., Zubowski, T., Rousseau, S., Dennis-Bohm, H., Galbraith, M., Fu, C., Hay, D., Degraaf, R., Barrs, J., Kelly, B., 2019. Proceedings of the National Workshop

on Filling in the Forage Fish Gap. Canadian Technical Report of Fisheries and Aquatic Sciences, 3287, pp. 82. ISBN 978-0-660-28642-6; ISSN 1488-5379.
Bouguet, J.Y., 2014. Camera Calibration Toolbox for Matlab. http://www.vision.caltech.edu/bouguetj/calib_doc/.
Boyd, C., Woillez, M., Bertrand, S., Castillo, R., Bertrand, A., Punt, A.E., 2015. Bayesian posterior prediction of the patchy spatial distributions of small pelagic fish in regions of suitable habitat. Can. J. Fish. Aquat. Sci. 72, 290–303.
Britt, L.L., Loew, E.R., McFarland, W.N., 2001. Visual pigments in the early life stages of Pacific northwest marine fishes. J. Exp. Biol. 204 (14), 2581–2587.
Brodeur, R.D., 2001. Habitat-specific distribution of Pacific ocean perch (*Sebastes alutus*) in Pribilof Canyon, Bering Sea. Cont. Shelf Res. 21 (3), 207–224.
Clarke, M.E., Tolimieri, N., Singh, H., 2009. Using the seabed AUV to assess populations of groundfish in untrawlable areas. In: Beamish, R.J., Rothschild, B.J. (Eds.), The Future of Fisheries Science in North America. Springer Science, p. 357.
De Robertis, A., Handegard, N.O., 2013. Fish avoidance of research vessels and the efficacy of noise-reduced vessels: a review. Ices J. Mar. Sci. 70 (1), 34–45.
Denney, C., Fields, R., Gleason, M., Starr, R., 2017. Development of new method for quantifying fish density using underwater stereo-video tools. J. Vis. Exp. 129 (e56625), 1–10.
Forland, T.N., Hobæk, H., Ona, E., Korneliussen, R.J., 2014. Broad bandwidth acoustic backscattering from sandeel—measurements and finite element simulations. Ices J. Mar. Sci. 71 (7), 1894–1903.
Fraser, H.M., Greenstreet, S.P., Piet, G.J., 2007. Taking account of catchability in groundfish survey trawls: implications for estimating demersal fish biomass. Ices J. Mar. Sci. 64 (9), 1800–1819.
Freeman, S., Mackinson, S., Flatt, R., 2004. Diel patterns in the habitat utilisation of sandeels revealed using integrated acoustic surveys. J. Exp. Mar. Biol. Ecol. 305 (2), 141–154.
Fréon, P., Misund, O.A., 1999. Dynamics of Pelagic Fish Distribution and Behavior: Effects on Fisheries and Stock Assessment. Blackwell Science, Oxford, UK.
Gaichas, S.K., Aydin, K.Y., Francis, R.C., 2010. Using food web model results to inform stock assessment estimates of mortality and production for ecosystem-based fisheries management. Can. J. Fish. Aquat. Sci. 67 (9), 1490–1506.
Gauthier, S., Horne, J.K., 2004. Acoustic characteristics of forage fish species in the Gulf of Alaska and Bering Sea based on Kirchhoff-approximation models. Can. J. Fish. Aquat. Sci. 61 (10), 1839–1850.
Gaydos, J.K., Pearson, S.F., 2011. Birds and mammals that depend on the Salish Sea: a compilation. Northwest. Nat. 92 (2), 79–95.
Gaydos, J.K., Dierauf, L., Kirby, G., Brosnan, D., Gilardi, K., Davis, G.E., 2008. Top 10 principles for designing healthy coastal ecosystems like the Salish Sea. EcoHealth 5 (4), 460.
Greene, H.G., Barrie, V., 2011. Potential Marine Benthic Habitats of the San Juan Archipelago. Geological Survey of Canada Marine Map Series, 4 Quadrants, 12 Sheets, Scale 1:50,000; Geological Survey of Canada: Sidney, BC, Canada, 2011.
Greene, H.G., Bizzarro, J.J., O'Connell, V.M., Brylinsky, C.K., 2007. Construction of digital potential marine benthic habitat maps using a coded classification scheme and its application. Mapp. Seafloor Habitat Charact. Can. Geol. Assoc. Spec. Pap. 47, 141–155.
Greene, H.G., Wyllie-Echeverria, T., Gunderson, D., Bizzarro, J., Barrie, V., Fresh, K., Robinson, C., Cacchione, D., Penttila, D., Hampton, M., 2011. Deep-Water Pacific Sand Lance (Ammodytes hexapterus) Habitat Evaluation and Prediction for the Northwest Straits Region; Final Report to Northwest Straits Commission. SeaDoc/Tombolo Mapping Lab and Friday Harbor Labs, Orcas Island, WA, USA, p. 21.
Greene, C., Kuehne, L., Rice, C., Fresh, K., Penttila, D., 2015. Forty years of change in forage fish and jellyfish abundance across greater Puget Sound, Washington (USA): anthropogenic and climate associations. Mar. Ecol. Prog. Ser. 525, 153–170.
Greene, H.G., Cacchione, D.A., Hampton, M.A., 2017. Characteristics and Dynamics of a Large Sub-tidal Sand Wave Field – Habitat for Pacific Sand Lance (*Ammodytes Personatus*). Salish Sea, Washington, USA.
Greene, H.G., Baker, M.R., Aschoff, J., 2020. A dynamic bedforms habitat for the forage fish pacific sand lance, San Juan Islands, WA, United States. Seafloor Geomorphology As Benthic Habitat. Elsevier, pp. 267–279.
Greene, H.G., Baker, M.R., Aschoff, J., Pacunski, R., 2021. Hazards evaluation of a valuable vulnerable sand-wave field forage fish habitat in the marginal central Salish Sea using a submersible. Oceanologia.
Greenstreet, S.P., Holland, G.J., Guirey, E.J., Armstrong, E., Fraser, H.M., Gibb, I.M., 2010. Combining hydroacoustic seabed survey and grab sampling techniques to assess "local" sandeel population abundance. Ices J. Mar. Sci. 67 (5), 971–984.
Hanselman, D.H., Spencer, P.D., McKelvey, D.R., Martin, M.H., 2012. Application of an acoustic–trawl survey design to improve estimates of rockfish biomass. Fish. Bull. 110 (4), 379–396.
Harvey, E., Cappo, M., Shortis, M., Robson, S., Buchanan, J., Speare, P., 2003. The accuracy and precision of underwater measurements of length and maximum body depth of southern bluefin tuna (*Thunnus maccoyii*) with a stereo-video camera system. Fish. Res. 63, 315–326.
Hassel, A., Knutsen, T., Dalen, J., Skaar, K., Østensen, Ø., Haugland, E.K., Fonn, M., 2003. Reaction of Sandeel to Seismic Shooting: a Field Experiment and Fishery Statistics Study. Institute of Marine Research, Norway.
Hassel, A., Knutsen, T., Dalen, J., Skaar, K., Løkkeborg, S., Misund, O.A., Østensen, Ø., Fonn, M., Haugland, E.K., 2004. Influence of seismic shooting on the lesser sandeel (*Ammodytes marinus*). Ices J. Mar. Sci. 61 (7), 1165–1173.
Haynes, T.B., Robinson, C.L.K., 2011. Re-use of shallow sediment patches by Pacific sand lance in Barkley Sound, British Columbia. Canada Environmental Biology of Fishes 92, 1–12.
Hilborn, R., 1979. Comparison of fisheries control systems that utilize catch and effort data. J. Fish Res. Board Can. 36, 1477–1489.
Hilborn, R., Walters, C.J., 2013. Quantitative Fisheries Stock Assessment: Choice, Dynamics and Uncertainty. Springer Science and Business Media.
Hobson, E.S., 1986. Predation on the Pacific sand lance, *Ammodytes hexapterus*, during the transition between day and night in southeastern Alaska. Copeia 1986 (1), 223–226.
Høines, Å.S., Bergstad, O.A., 2001. Density of wintering sand eel in the sand recorded by grab catches. Fish. Res. 49 (3), 295–301.
Honkalehto, T., Ressler, P.H., Towler, R.H., Wilson, C.D., 2011. Using acoustic data from fishing vessels to estimate walleye pollock (*Theragra chalcogramma*) abundance in the eastern Bering Sea. Can. J. Fish. Aquat. Sci. 68 (7), 1231–1242.
Horne, J.K., 2000. Acoustic approaches to remote species identification: a review. Fish. Oceanogr. 9, 356–371.
ICES, 2008. Report of the ICES Advisory Committee, 2008. Book 6. North Sea (pg. 50-53).
Jensen, H., 2001. Settlement Dynamics in the Lesser Sandeel *Ammodytes marinus* in the North Sea. PhD thesis. University of Aberdeen.
Johnsen, E., Pedersen, R., Ona, E., 2009. Size-dependent frequency response of sandeel schools. Ices J. Mar. Sci. 66, 1100–1105.
Karp, M.A., Peterson, J.O., Lynch, P.D., Griffis, R.B., Adams, C.F., Arnold, W.S., Barnett, L.A.K., deReynier, Y., DiCosimo, J., Fenske, K.H., Gaichas, S.K., Hollowed, A., Holsman, K.K., Karnauskas, M., Kobayashi, D., Leising, A., Manderson, J.P., McClure, M., Morrison, W.E., Schnettler, E., Thompson, A., Thorson, J.T., Walter 3rd, J.F., Yau, A.J., Methot, R.D., Link, J.S., 2019. Accounting for shifting distributions and changing productivity in the development of scientific advice for fishery management. Ices J. Mar. Sci. 76 (5), 1305–1315.
Koslow, J.A., Davison, P.C., 2016. Productivity and biomass of fishes in the California current large marine ecosystem: comparison of fishery-dependent and-independent time series. Environ. Dev. 17, 23–32.
Koslow, J.A., Kloser, R., Stanley, C.A., 1995. Avoidance of a camera system by a deepwater fish, the orange roughy (*Hoplostethus atlanticus*). Deep. Sea Res. Part I Oceanogr. Res. Pap. 42 (2), 233–244.
Krieger, K., Heifetz, J., Ito, D., 2001. Rockfish assessed acoustically and compared to bottom-trawl catch rates. Alaska Fishery Research Bulletin 8 (1), 71–77.
Kubilius, R., Ona, E., 2012. Target strength and tilt-angle distribution of lesser sandeel (*Ammodytes marinus*). Ices J. Mar. Sci. 69, 1099–1107.
Laidig, T.E., Krigsman, L.M., Yoklavich, M.M., 2013. Reactions of fishes to two underwater survey tools, a manned submersible and a remotely operated vehicle. Fish. Bull. 111 (1), 54–67.
Liedtke, T., Gibson, C., Lowry, D., Fagergren, D., 2013. Conservation and Ecology of Marine Forage Fishes—Proceedings of a Research Symposium, September 2012. U.S. Geological Survey Open-File Report 2013-1035.
Link, J.S., Nye, J.A., Hare, J.A., 2011. Guidelines for incorporating fish distribution shifts into a fisheries management context. Fish Fish. 12 (4), 461–469.
Mackinson, S., Turner, K., Righton, D., Metcalfe, J.D., 2005. Using acoustics to investigate changes in efficiency of a sandeel dredge. Fish. Res. 71, 357–363.
Matta, M.E., Baker, M.R., 2020. Age and growth of Pacific sand lance (*Ammodytes personatus*) at the latitudinal extremes of the Gulf of Alaska large marine ecosystem. Northwest Nat (Olymp. Wash.) 101 (1).
Maunder, M.N., Punt, A.E., 2004. Standardizing catch and effort data: a review of recent approaches. Fish. Res. 70 (2-3), 141–159.
McGowan, D.W., Horne, J.K., Thorson, J.T., Zimmermann, M., 2019. Influence of environmental factors on capelin distributions in the Gulf of Alaska. Deep. Sea Res. Part Ii Top. Stud. Oceanogr. 165, 238–254.
McIntyre, F.D., Neat, F., Collie, N., Stewart, M., Fernandes, P.G., 2015. Visual surveys can reveal rather different 'pictures' of fish densities: comparison of trawl and video camera surveys in the Rockall Bank, NE Atlantic Ocean. Deep-Sea Research 95, 67–74.
Millar, R.B., Methot, R.D., 2002. Age-structured meta-analysis of US West Coast rockfish (Scorpaenidae) populations and hierarchical modeling of trawl survey catchabilities. Can. J. Fish. Aquat. Sci. 59 (2), 383–392.
Moriarty, M., Sethi, S.A., Pedreschi, D., Smeltz, T.S., McGonigle, C., Harris, B.P., Wolf, N., Greenstreet, S.P., 2020. Combining fisheries surveys to inform marine species distribution modelling. ICES J. Mar. Sci. 77 (2), 539–552.
Mosteiro, A., Fernandes, P.G., Armstrong, F., Greenstreet, S.P.R., 2004. A dual frequency algorithm for the identification of sandeel school echotraces. ICES Document CM 12, 1–13.
Muggeo, V.M.R., 2003. Estimating regression models with unknown break-points. Stat. Med. 22, 3055–3071.
Muggeo, V.M.R., 2008. Segmented: an R Package to Fit Regression Models With Broken-line Relationships. R News 8/1, pp. 20–25.
Muhling, B., Brodie, S., Snodgrass, O., Tommasi, D., Dewar, H., Childers, J., Jacox, M., Edwards, C.A., Xu, Y., Snyder, S., 2019. Dynamic habitat use of albacore and their primary prey species in the California current System. California Cooperative Oceanic Fisheries Investigations Report 60, 79–93.
Nasby-Lucas, N.M., Embley, B.W., Hixon, M.A., Merle, S.G., Tissot, B.N., Wright, D.J., 2002. Integration of submersible transect data and high-resolution multibeam sonar imagery or a habitat-based groundfish assessment of Heceta Bank, Oregon. Fish. Bull. 100, 739–751.
Newton, J.A., Baker, M.R., Tyler, W.B., 2018. San Juan pelagic ecosystem – a 15 year perspective. In: Moore, S.K., Wold, R., Curry, B., Stark, K., Bos, J., Williams, P., Hamel, N., Apple, J., Kim, S., Brown, A., Krembs, C., Newton, J. (Eds.), PSEMP Marine Waters Workgroup. Puget Sound Marine Waters: 2018 Overview. www.psp.wa.gov/PSmarinewatersoverview.php.
Newton, J.A., Baker, M.R., Guenther, R., Tyler, W.B., 2019. San Juan channel and Juan de fuca surveys. In: Moore, S.K., Wold, R., Stark, K., Bos, J., Williams, P., Hamel, N., Kim, S., Brown, A., Krembs, C., Newton, J. (Eds.), PSEMP Marine Waters Workgroup.

Puget Sound Marine Waters: 2019 Overview. www.psp.wa.gov/PSmarinewatersoverview.php.
Ona, E., Mitson, R.B., 1997. Acoustic sampling and signal processing near the seabed: the deadzone revisited. Oceanographic Literature Review 3 (44), 279.
Ormseth, O.A., Rand, K.M., De Robertis, A., 2017. Fishes and Invertebrates in Gulf of Alaska Bays and Islands: Results From Inshore Ecosystem Surveys in 2011 and 2013. U.S. Dep. Commer., NOAA Tech. Memo. NMFS-AFSC-344, 140 p. https://apps-afsc.fisheries.noaa.gov/Publications/AFSC-TM/NOAA-TM-AFSC-344.pdf.
Ormseth, O.A., Baker, M.R., Hopcroft, R.R., Ladd, C., Mordy, C.W., Moss, J.H., Mueter, F. J., Shotwell, S.K., Strom, S.L., 2019. Introduction to understanding ecosystem processes in the Gulf of Alaska, volume 2. Deep Sea Res. Part II 165, 1–6.
Orr, J.W., Wildes, S., Kai, Y., Raring, N., Nakabo, T., Katugin, O., Guyon, J., 2015. Systematics of North Pacific sand lances of the genus *Ammodytes* based on molecular and morphological evidence, with the description of a new species from Japan. Fish. Bull. 113 (2).
Ostrand, W.D., Gotthardt, T.A., Howlin, S., Robards, M.D., 2005. Habitat selection models for Pacific sand lance (*Ammodytes hexapterus*) in Prince William Sound, Alaska. Northwest. Nat. 86 (3), 131–143.
Pacunski, R.E., Palsson, W.A., Greene, H.G., Gunderson, D., 2008. Conducting Visual Surveys With a Small ROV in Shallow Water. Marine Habitat Mapping Technology for Alaska, pp. 109–128.
Pacunski, R.E., Palsson, W.A., Greene, H.G., 2013. Estimating Fish Abundance and Community Composition on Rocky Habitats in the San Juan Islands Using a Small Remotely Operated Vehicle. Washington Department of Fish and Wildlife, Fish Program Fish Management Division, 600 Capitol Way N., Olympia, WA 98501.
Pietsch, T.W., Orr, J.W., 1999. Fishes of the Salish Sea; a Compilation and Distributional Analysis. U.S. Department of Commerce. NOAA Professional Paper NMFS 18, 106 p. doi:10.7755/ PP.18.
Robards, M.D., Anthony, J.A., Rose, G.A., Piatt, J.F., 1999. Changes in proximate composition and somatic energy content for Pacific sand lance (*Ammodytes hexapterus*) from Kachemak Bay, Alaska relative to maturity and season. Journal of Experimental Marine Biology and Cology 242 (2), 245–258.
Rodgveller, C.J., Sigler, M.F., Hanselman, D.H., Ito, D.H., 2011. Sampling efficiency of longlines for Shortraker and Rougheye Rockfish using observations from a manned submersible. Mar. Coast. Fish. Dyn. Manag. Ecosyst. Sci. 3 (1), 1–9.
Rooper, C.N., Hoff, G.R., De Robertis, A., 2010. Assessing habitat utilization and rockfish (*Sebastes* spp.) biomass on an isolated rocky ridge using acoustics and stereo image analysis. Can. J. Fish. Aquat. Sci. 67, 1658–1670.
Rooper, C.N., Williams, K., De Robertis, A., Tuttle, V., 2015. Effect of underwater lighting on observations of density and behavior of rockfish during camera surveys. Fish. Res. 172, 157–167.
Rooper, C.N., Williams, K., Towler, R.H., Wilborn, R., Goddard, P., 2020. Estimating habitat-specific abundance and behavior of several groundfishes using stationary stereo still cameras in the southern California bight. Fish. Res. 224, 105443.
Ryer, C.H., Stoner, A.W., Iseri, P.J., Spenser, M.L., 2009. Effects of simulated underwater vehicle lighting on fish behavior. Mar. Ecol. Prog. Ser. 391, 97–106.
Sainsbury, K.J., Punt, A.E., Smith, A.D., 2000. Design of operational management strategies for achieving fishery ecosystem objectives. Ices J. Mar. Sci. 57 (3), 731–741.
Seiler, J., Williams, A., Barrett, N., 2012. Assessing size, abundance and habitat preferences of the Ocean Perch (*Helicolenus percoides*) using a AUV-borne stereo camera system. Fish. Res. 129, 64–72.
Selleck, J.R., Gibson, C.F., Shull, S., Gaydos, J.K., 2015. Nearshore distribution of Pacific sand lance (*Ammodytes personatus*) in the inland waters of Washington State. Northwest. Nat. 185–195.
Shortis, M.R., Seager, J.W., Williams, A., Barker, B.A., Sherlock, M., 2009. Using stereo video for deep water benthic habitat surveys. Marine Technological Soc. J. 42, 28–37.
Sisson, N.B., Baker, M.R., 2017. Feeding ecology of pacific sand lance in the San Juan Archipelago. Mar. Coast. Fish. Dyn. Manag. Ecosyst. Sci. 9 (1), 612–625.
Somerton, D.A., Williams, K., Campbell, M.D., 2017. Quantifying the behavior of fish in response to a moving camera vehicle by using benthic stereo cameras and target tracking. Fish. Bull. 115, 343–354.
Spencer, P.D., Ianelli, J.N., 2014. Assessment of the Northern Rockfish Stock in the Eastern Bering Sea and Aleutian Islands. Stock Assessment and Fishery Evaluation Report for the Groundfish Resources of the Bering Sea/Aleutian Islands Regions, pp. 1395–1451.
Starr, R.M., Fox, D.S., Hixon, M.A., Tissot, B.N., Johnson, G.E., Barss, W.H., 1996. Comparison of submersible-survey and hydroacoustic-survey estimates of fish density on a rocky bank. Fish. Bull. 94, 113–123.
Stein, D., Tissot, B.N., Hixon, M.A., Barss, W., 1992. Fish-habitat associations on a deep reef at the edge of the Oregon continental shelf. Fish. Bull. 90, 540–551.
Stoner, A.W., Ryer, C.H., Parker, S.J., Auster, P.J., Wakefield, W.W., 2008. Evaluating the role of fish behavior in surveys conducted with underwater vehicles. Can. J. Fish. Aquat. Sci. 65, 1230–1243.
Thomson, R.E., Ware, D.M., 1996. A current velocity index of ocean variability. J. Geophys. Res. Oceans 101 (C6), 14297–14310.
Thorson, J.T., Ward, E.J., 2014. Accounting for vessel effects when standardizing catch rates from cooperative surveys. Fish. Res. 155, 168–176.
Thorson, J.T., Stewart, I.J., Punt, A.E., 2011. Accounting for fish shoals in single-and multi-species survey data using mixture distribution models. Can. J. Fish. Aquat. Sci. 68 (9), 1681–1693.
Thorson, J.T., Fonner, R., Haltuch, M.A., Ono, K., Winker, H., 2016. Accounting for spatiotemporal variation and fisher targeting when estimating abundance from multispecies fishery data. Can. J. Fish. Aquat. Sci. 74 (11), 1794–1807.
Tokranov, A.M., 2007. Distribution and some biological features of the Pacific sand lance (*Ammodytes hexapterus)* in waters off Kamchatka in the Sea of Okhotsk. J. Ichthyol. 47 (4), 288–295.
Tolimieri, N., Clarke, M.E., Singh, H., Goldfinger, C., 2008. Evaluating the SeaBD AUV for monitoring groundfish in untrawlable habitat. In: Reynolds, J.R., Greene, H.G. (Eds.), Marine Habitat Mapping Technology for Alaska. University of Alaska Fairbanks. https://doi.org/10.4027/mhmta.2008.09. Alaska Sea Grant.
Trenkel, V.M., Lorance, P., Mahevés, S., 2004. Do visual transects provide true population density estimates for deepwater fish? Ices J. Mar. Sci. 61, 1050–1056.
van der Kooij, J., Scott, B.E., Mackinson, S., 2008. The effects of environmental factors on daytime sandeel distribution and abundance on the Dogger Bank. J. Sea Res. 60 (3), 201–209.
van Deurs, M., Christiansen, A., Frisk, C., Mosegaard, H., 2010. Overwintering strategy of sandeel ecotypes from an energy/predation trade-off perspective. Mar. Ecol. Prog. Ser. 416, 201–214.
van Deurs, M., Grome, T.M., Kaspersen, M., Jensen, H., Stenberg, C., Sørensen, T.K., Støttrup, J., Warnar, T., Mosegaard, H., 2012. Short-and long-term effects of an offshore wind farm on three species of sandeel and their sand habitat. Mar. Ecol. Prog. Ser. 458, 169–180.
Ward, P., 2008. Empirical estimates of historical variations in the catchability and fishing power of pelagic longline fishing gear. Rev. Fish Biol. Fish. 18 (4), 409–426.
Watson, D.L., Harvey, E.S., Anderson, M.J., Kendrick, G.A., 2005. A comparison of temperate reef fish assemblages recorded by three underwater stereo-video techniques. Mar. Biol. 148, 415–425.
Williams, K., Rooper, C.N., Towler, R., 2010. Use of stereo camera systems for assessment of rockfish abundance in untrawlable areas and for recording pollock behavior during midwater trawls. Fish. Bull. 108 (3), 352–362.
Williams, K., De Robertis, A., Berkowitz, Z., Rooper, C., Towler, R., 2014. An underwater stereo-camera trap. Methods Oceanogr. 11, 1–2.
Williams, K., Towler, R., Goddard, P., Wilborn, R., Rooper, C., 2016a. SEBASTES Stereo Image Analysis Software. FSC Processed Report 2016-03. Alaska Fisheries Science Center, NOAA, Seattle, WA. https://doi.org/10.7289/V5/AFSC-PR-2016-03. In: http://www.afsc.noaa.gov/Publications/ProcRpt/PR2016-03.pdf.
Williams, K., Lauffenburger, N., Chuang, M.C., Hwang, J.N., Towler, R., 2016b. Automated measurements of fish within a trawl using stereo images from a Camera-Trawl device (CamTrawl). Methods Oceanogr. 17, 138–152.
Williams, K., Rooper, C.N., De Robertis, A., Levine, M., Towler, R., 2018. A method for computing volumetric fish density using stereo cameras. J. Exp. Mar. Biol. Ecol. 508, 21–26.
Winslade, P., 1974. Behavioural studies on the lesser sandeel *Ammodytes marinus* (Raitt) III. The effect of temperature on activity and the environmental control of the annual cycle of activity. J. Fish Biol. 6 (5), 587–599.
Wright, P.J., Jensen, H., Tuck, I., 2000. The influence of sediment type on the distribution of the Lesser Sandeel, *Ammodytes marinus*. J. Sea Res. 44, 243–256.
Yoklavich, M.M., Cailliet, G.M., Barry, J.P., Ambrose, D.A., Antrim, B.S., 1991. Temporal and spatial patterns in abundance and diversity of fish assemblages in Elkhorn Slough, California. Estuaries 14 (4), 465–480.
Yoklavich, M.M., Greene, H.G., Cailliet, G.M., Sullivan, D.E., Lea, R.N., Love, M.S., 2000. Habitat associations of deep-water rockfishes in a submarine canyon: an example of a natural refuge. Fish. Bull. U.S. 98, 625–641.
Yoklavich, M.M., Love, M.S., Forney, K.A., 2007. A fishery-independent assessment of an overfished rockfish stock, cowcod (*Sebastes levis*), using direct observations from an occupied submersible. Can. J. Fish. Aquat. Sci. 64 (12), 1795–1804.
Zimmermann, M., Prescott, M.M., Haeussler, P.J., 2019. Bathymetry and geomorphology of Shelikof Strait and the Western Gulf of Alaska. Geosciences 9 (10), 409.